LA-UR- 10-01117

Approved for public release; distribution is unlimited.

Title:	Proton Radiography: Studying Dynamic Properties of Shock-Loaded Materials
Author(s):	Cynthia Schwartz et al.
Intended for:	Future meetings

Los Alamos
NATIONAL LABORATORY
EST. 1943

Los Alamos National Laboratory, an affirmative action/equal opportunity employer, is operated by the Los Alamos National Security, LLC for the National Nuclear Security Administration of the U.S. Department of Energy under contract DE-AC52-06NA25396. By acceptance of this article, the publisher recognizes that the U.S. Government retains a nonexclusive, royalty-free license to publish or reproduce the published form of this contribution, or to allow others to do so, for U.S. Government purposes. Los Alamos National Laboratory requests that the publisher identify this article as work performed under the auspices of the U.S. Department of Energy. Los Alamos National Laboratory strongly supports academic freedom and a researcher's right to publish; as an institution, however, the Laboratory does not endorse the viewpoint of a publication or guarantee its technical correctness.

Form 836 (7/06)

Proton Radiography: Studying Dynamic Properties of Shock-Loaded Materials

The Proton Radiography facility at LANSCE (pRad) uses the unique features of high energy protons to generate multiple frame movies of dynamic experiments, typically driven by high explosives or gun shots. The high penetrating powers and low backgrounds associated with high energy protons, as well as the capability of a linear accelerator such as LANSCE to continuously generate flash proton pulses, make pRad a useful tool for studying several classes of dynamic experiments. Typical experiments include material failures under dynamic loads, such as shear band failure; nonlinear jet growth, including Richtmyer-Meshkov Instability growth; and material equation of state studies in shocked or other high pressure situations. The experimental techniques underlying pRad and examples of each of the above classes of experiments will be presented.

Proton Radiography: Studying Dynamic Properties of Shock-Loaded Materials

Cynthia L. Schwartz
and the pRad Collaboration
Physics Division
Los Alamos National Laboratory

5×10^6 Hz
800 MeV p

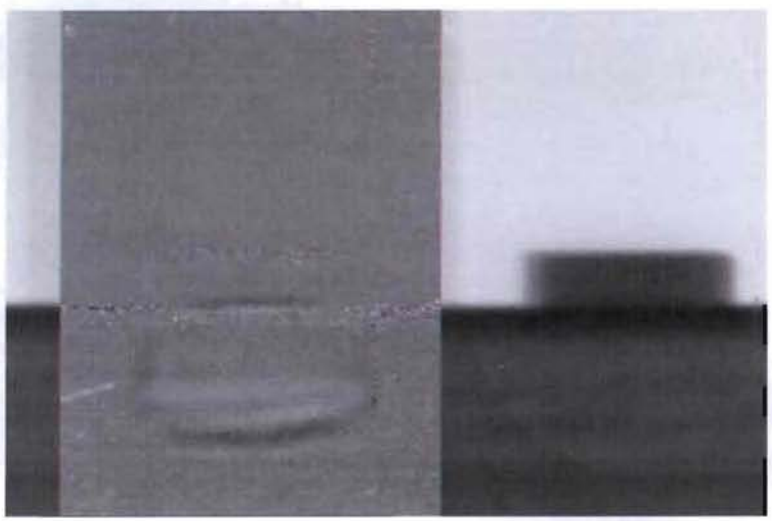

2 Hz
800 MeV p

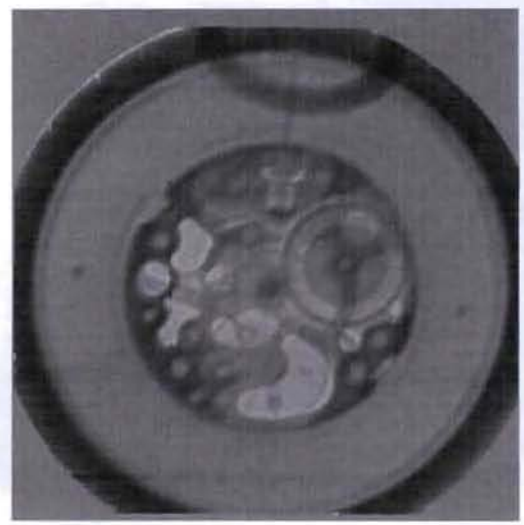

pRad Core Team

P-25

Eduardo Campos, Camilo Espinoza, Gary Hogan, Brian Hollander, Julian Lopez, Fesseha Mariam, Frank Merrill, Christopher Morris, Matthew Murray, Alexander Saunders, Cynthia Schwartz, T. Neil Thompson, Dale Tupa

DE-3

Joe Bainbridge, Robert Lopez, Mark Marr-Lyon, Paul Rightley

HX-4

Wendy McNeil

P-23

Gary Grim, Nicholas King, Kris Kwiatkowski, Paul Nedrow

LANSCE-NS

Leo Bitteker

NSTech

Douglas Lewis, Josh Tybo

LANSCE Experimental Areas

- Lujan Center
  - ***National security research***
  - ***Materials, bio-science, and nuclear physics***
  - ***National user facility***
- WNR
  - ***National security research***
  - ***Nuclear Physics***
  - ***Neutron Irradiation***
- Proton Radiography
  - ***National security research***
  - ***Dynamic Materials science,***
  - ***Hydrodynamics***
- Isotope Production Facility
  - ***Medical radioisotopes***

Proton Interactions

Proton Radiography

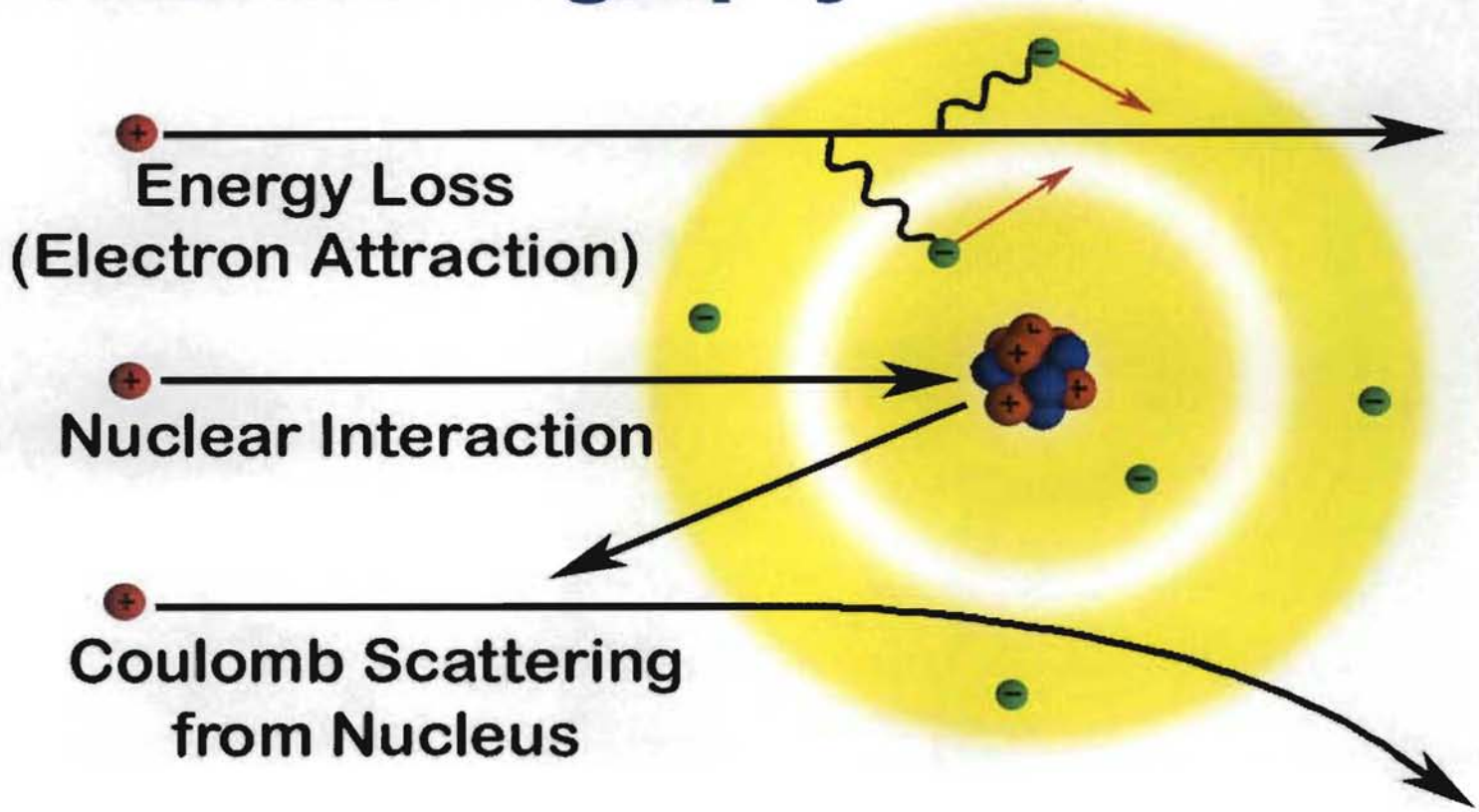

The idea-focus the transmitted protons with magnetic lenses

Transmission radiography FY95

with 188 MeV protons

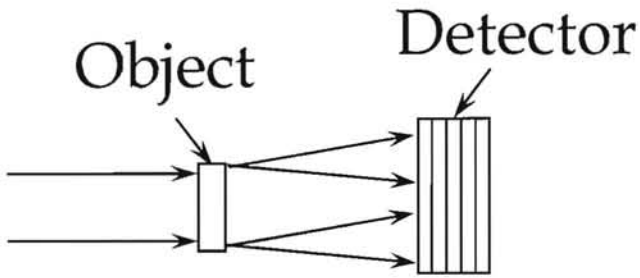

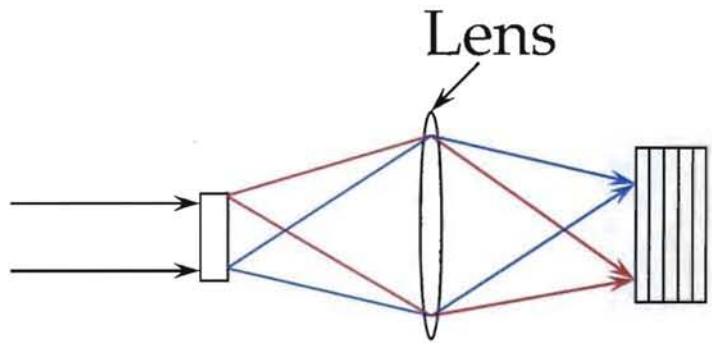

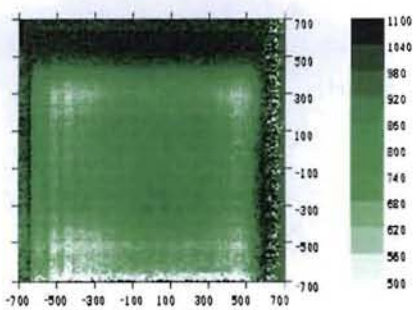

At the detector

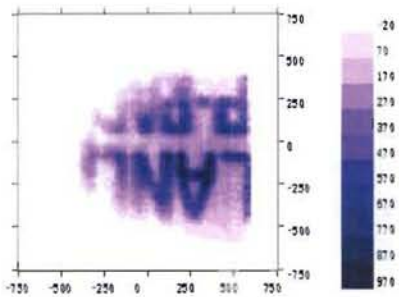

After a lens

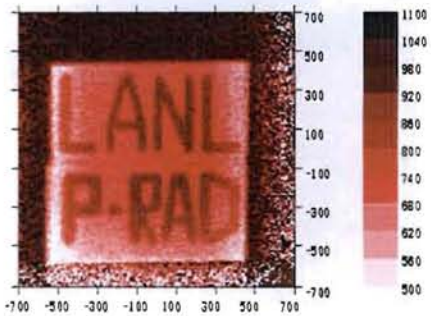

Projected to the object

Magnetic Imaging Lens

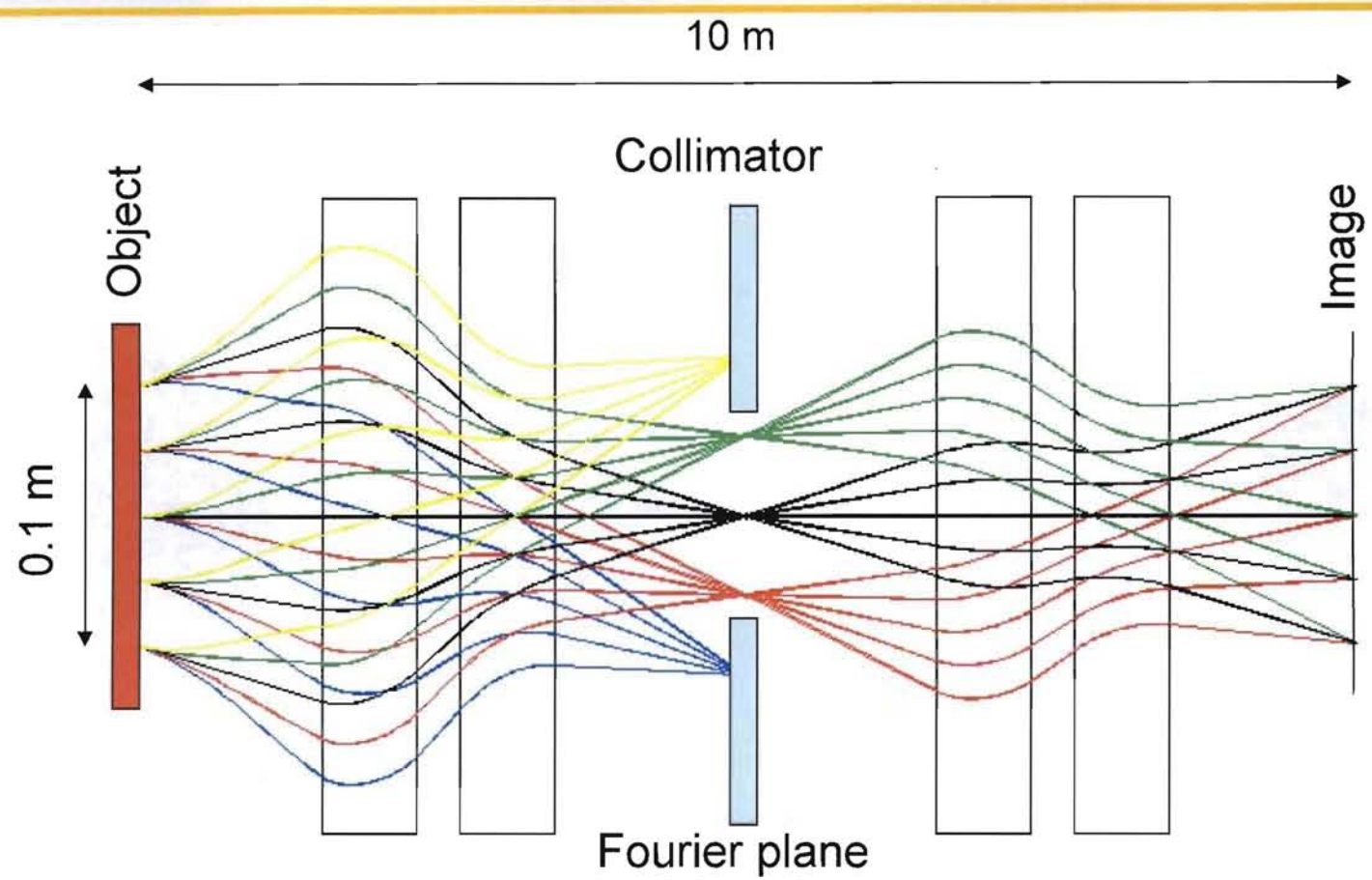

Quadrupole Identity Lens

Los Alamos
NATIONAL LABORATORY
EST. 1943
Operated by the Los Alamos National Security, LLC for the DOE/NNSA
NNSA

* C.T. Mottershead and J. D. Zumbro, "Magnetic Optics for Proton Radiography", Proceedings of the 1997 Particle Accelerator Conference

"Matching Miracle"

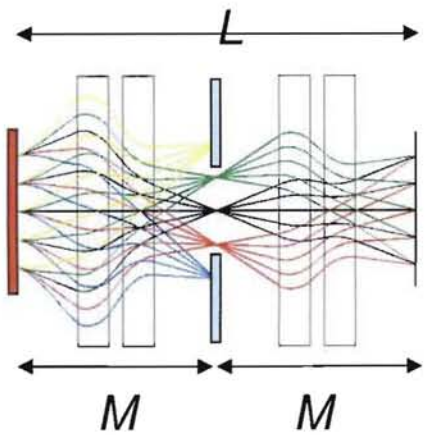

x_o, x_o' - position and angle at object
x_{fp} - position at midpoint of lens
x_i - position and angle at image
δ - $\Delta p/p$
M - Transport matrix for doublet
L - First order Transport matrix
T - Second order Transport tensor

$$L = M^2 = -I$$

Form identity lens from identical doublets

Fourier Plane

$$x_{fp} = M_{11}x_o + M_{12}x_o'$$
$$x_o' = wx_o + \phi$$
$$x_{fp} = M_{11}x_o + M_{12}(wx_o + \phi)$$
$$w = -M_{11}/M_{12}$$
$$x_{fp} = M_{12}\phi$$

Inject beam with position-angle correlation to form Fourier plane at center of lens.

Resolution

$$x_i = L_{11}x_o + L_{12}x_o' + T_{116}x_o\delta + T_{126}x_o'\delta$$
$$x_i = -x_o + T_{116}x_o\delta + T_{126}(wx_o + \phi)\delta$$
$$w = -T_{116}/T_{126} = -M_{11}/M_{12} \quad *$$
$$w = -M_{11}/M_{12}$$
$$\Delta x_i = T_{126}\phi\delta$$

Dominates Blur

Same position-angle correlation which forms a Fourier plane at the center of the magnet also cancels second order chromatic terms.

Contrast from Multiple Coulomb Scattering

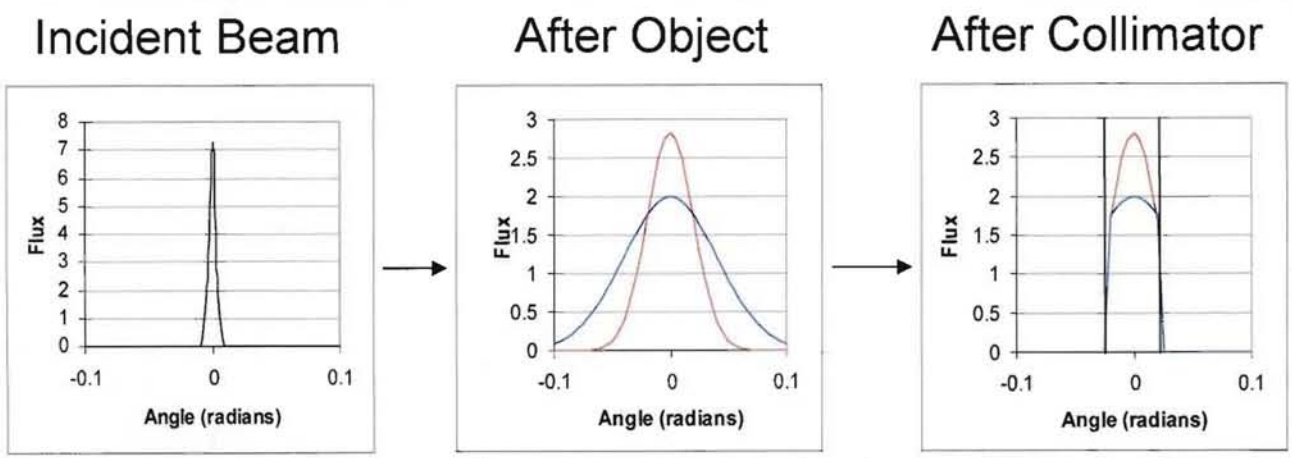

Measured transmission provides information of object thickness

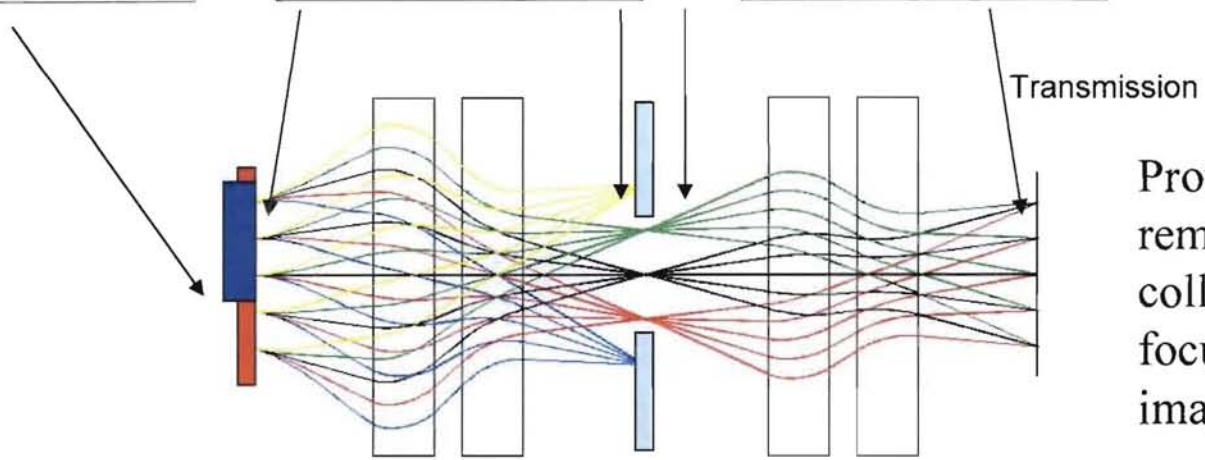

Protons not removed by collimator are re-focused at the image location.

Areal Density Reconstruction

$$T_{nuclear} = e^{-x/\lambda}$$

Nuclear removal processes

$$T_{MCS} = 1 - e^{-\theta_c^2 / 2\theta_o^2}$$

$$\theta_o = \frac{14.1 MeV}{p\beta}\sqrt{\frac{x}{x_o}}$$

Multiple Coulomb Scattering with collimation:

θ_o - scattering angle (radians)
x - areal density
x_o - radiation length
p - momentum (MeV)
β - relativistic velocity

$$T = e^{-x/\lambda}\left(1 - e^{-\left(\frac{\theta_c p\beta}{14.1\,MeV}\right)^2 \frac{x_o}{2x}}\right)$$

Total Transmission
- inverted to determine areal density, x

pRad Facility at LANSCE

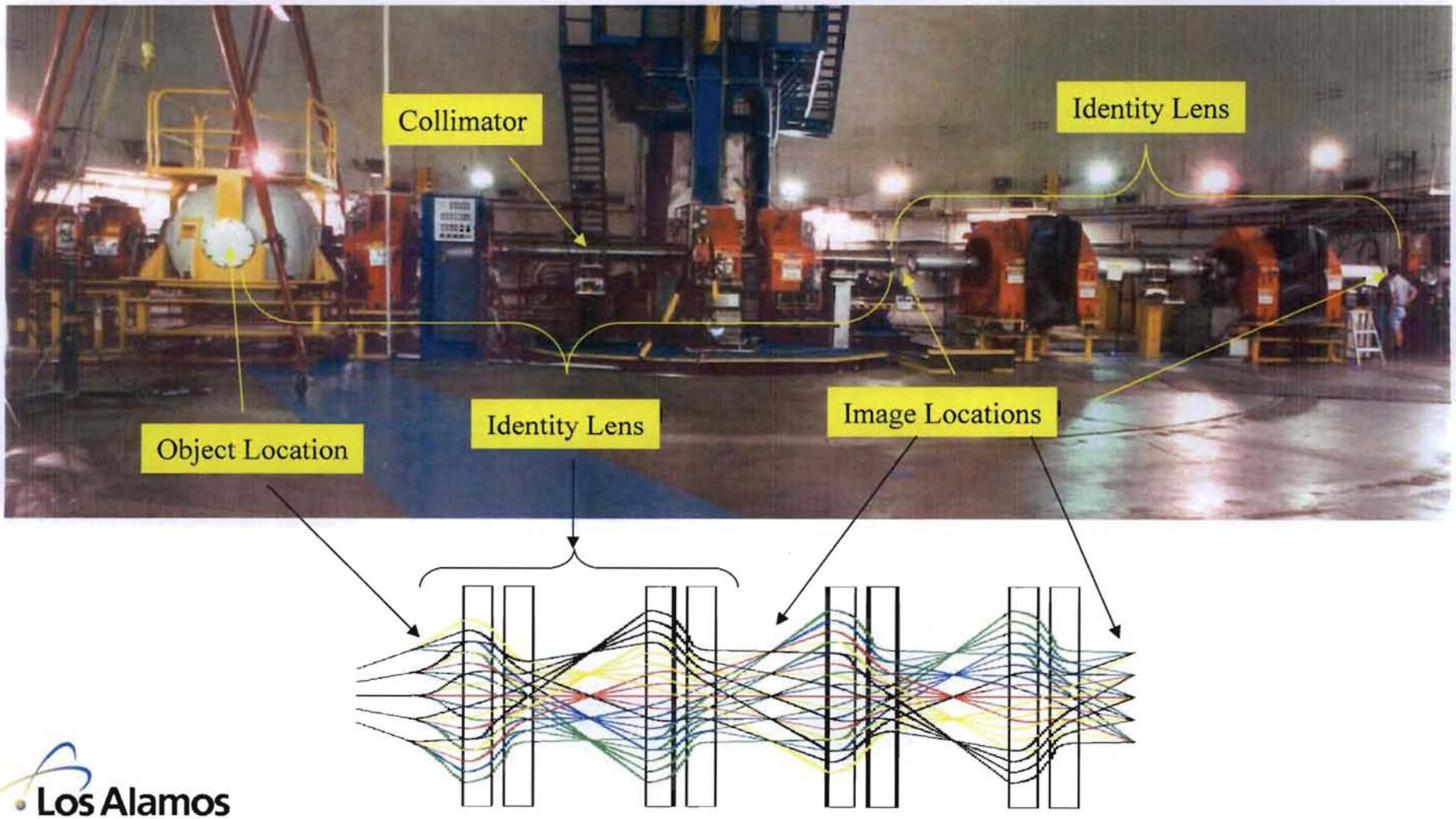

800 MeV Spatial Resolution

Identity Lens

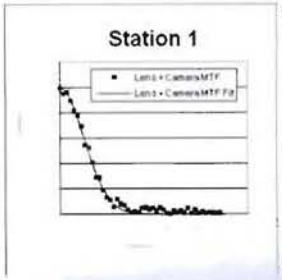

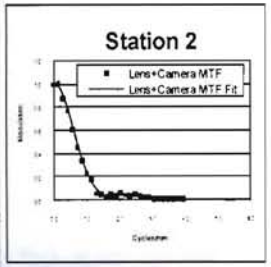

- Station 1: 178 μm
- 120 mm field of view

X3 Magnifier

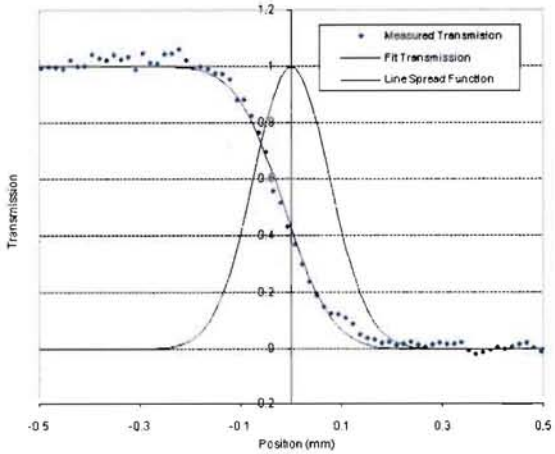

2.5 lp/mm

- Station 1: 65 μm
- 44 mm field of view

X7 Lens

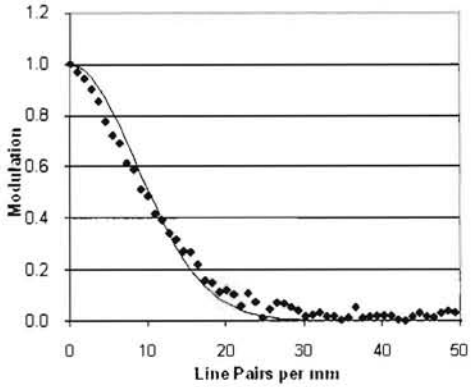

- Station 1: 30 μm
- 17 mm field of view

Temporal Resolution

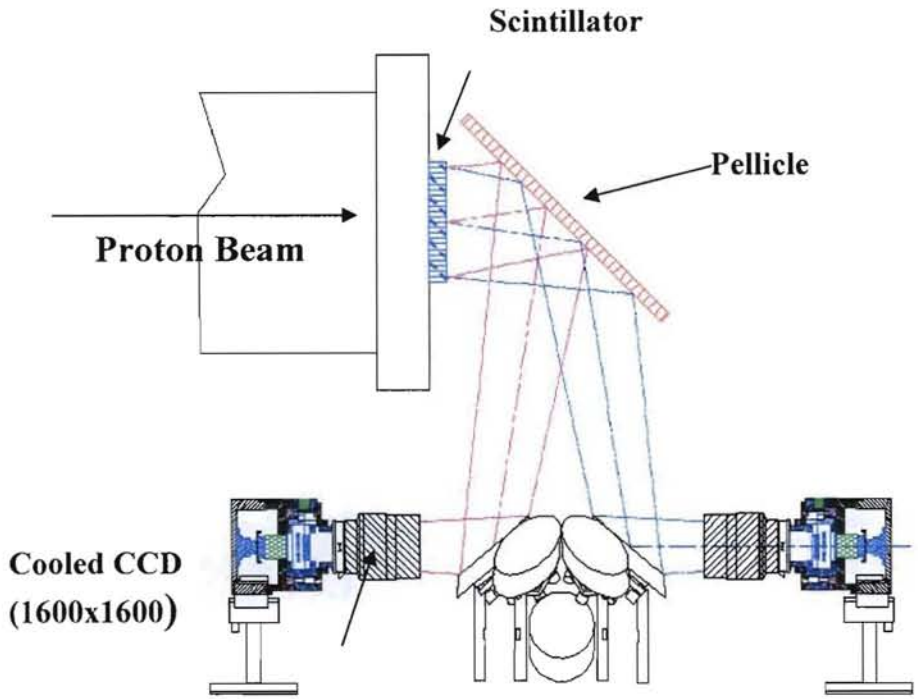

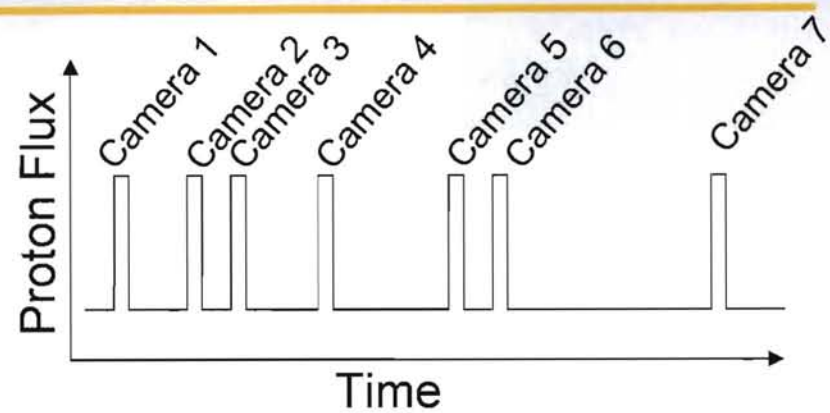

- **19** images at first station
- **22** images at second station
- Total **41** possible image times
- Typically **50 ns** exposure times

First 720×726-Pixel Hybrid Chip

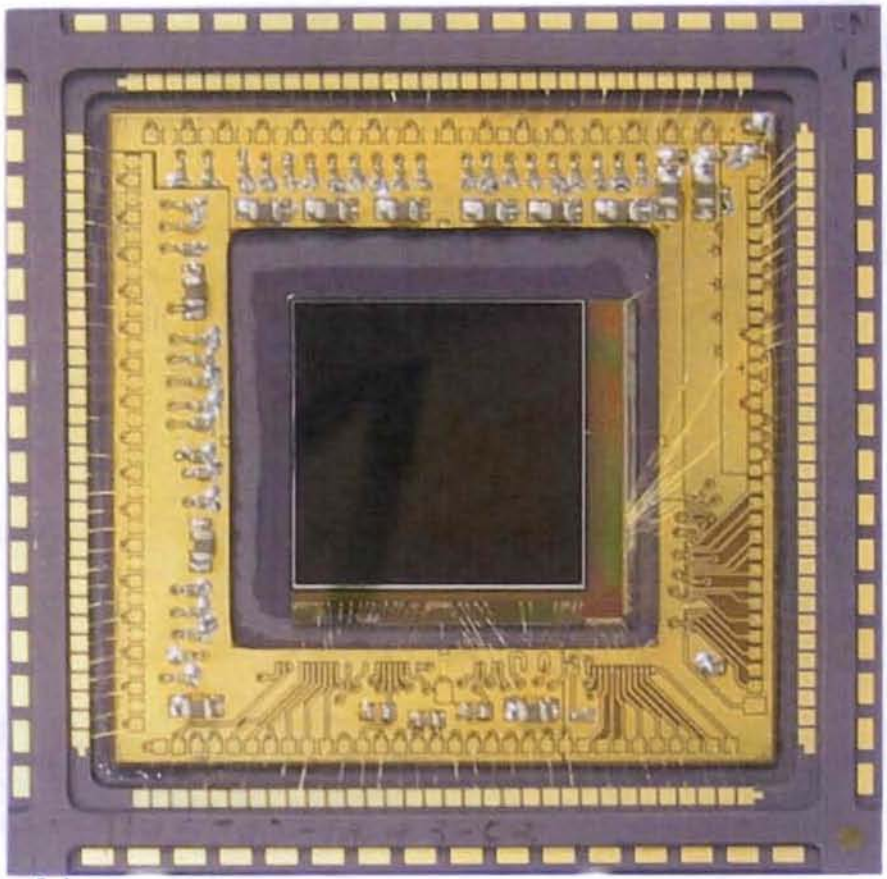

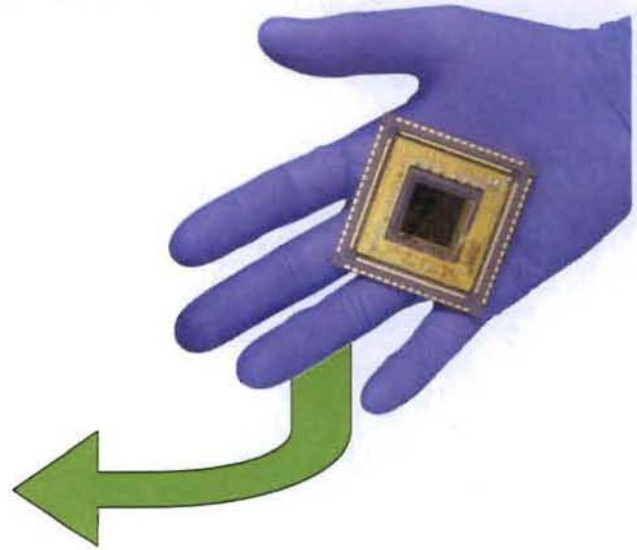

- Packaged prototype is a single 720 × 720px FPA
- 1440×1440 imager can use a 2-side buttable 720×726 FPA in a Tiled Assembly
- On and off-chip decoupling with multiple wire-bonds to dampen large power transients

Imager as Two-Component Hybrid Focal Plane Array (FPA)

- **Independent optimization of detector and readout IC**
- **~100% optical fill factor**
- **Arbitrarily large well depth**

(1) Photo-Diode Pixel Array (photon-charge conversion)

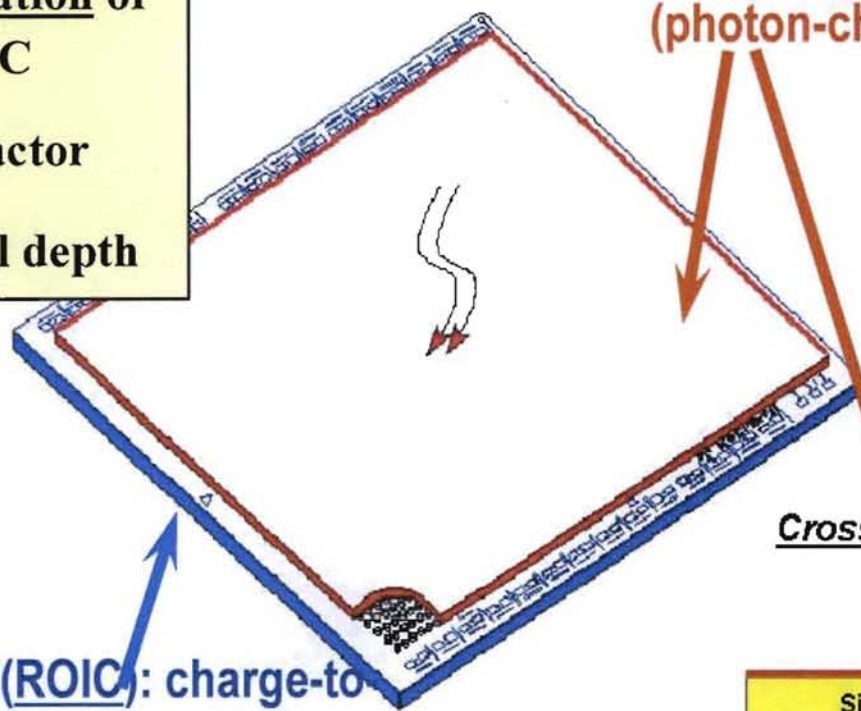

Cross-Sectional View

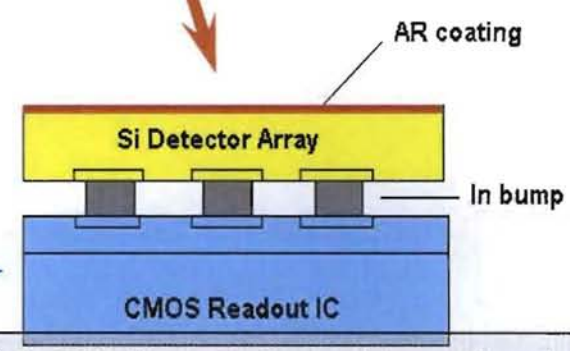

(2) CMOS Readout IC (ROIC): charge-to-voltage conversion, signal storage & processing, logic and A/D conversion;
SoC: photons-to-bits

Each pixel in PD Sensor Array bump bonded to corresponding pixel in ROIC

Rockwell/ Teledyne pRAD Cameras

Prototype –in Al housing

(Sizable volume taken-up by TEC cooler and fan)

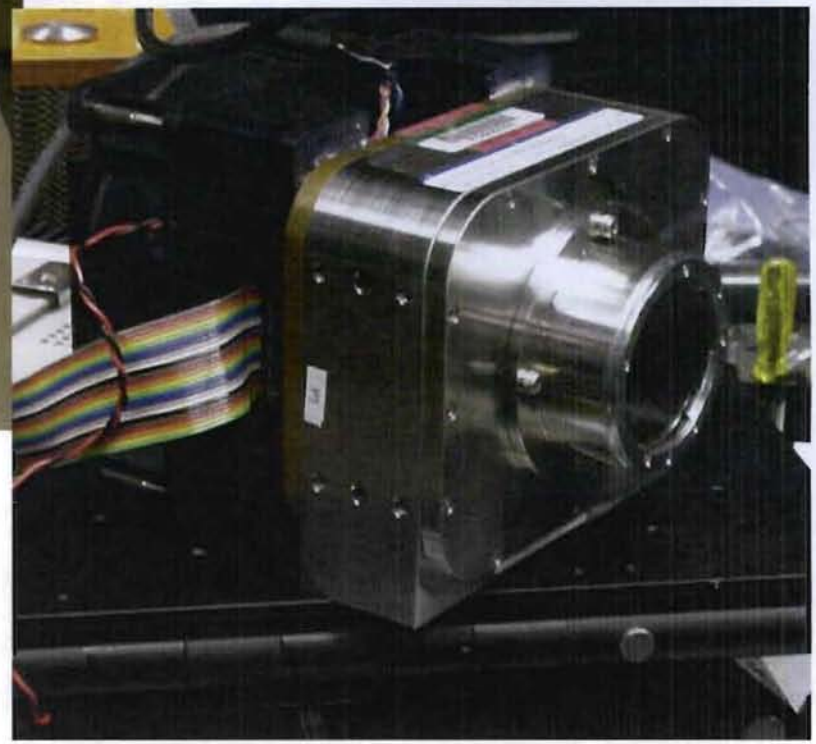

Stainless-Steel Dewar

Proton Radiograph Captures Fragmentation over Time

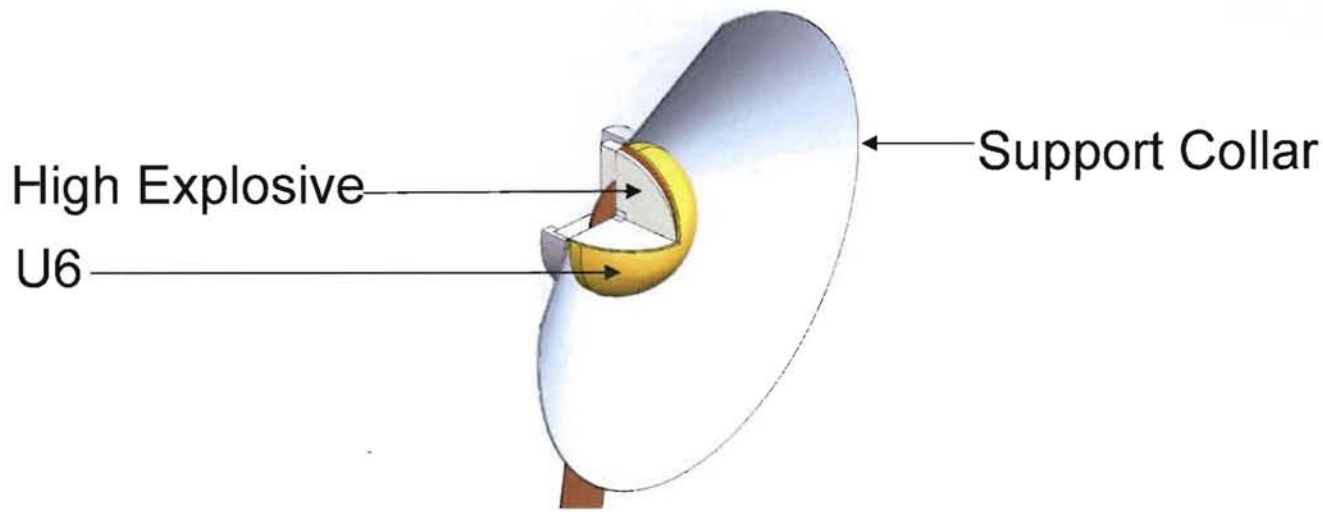

- Hemisphere of U6 is explosively expanded.
- Proton radiograph captures fragmentation over time
- Percent open/closed area is calculated from 100 random locations
- Support vector machine is used to categorize entire data set

Shear Band Failure in U6Nb

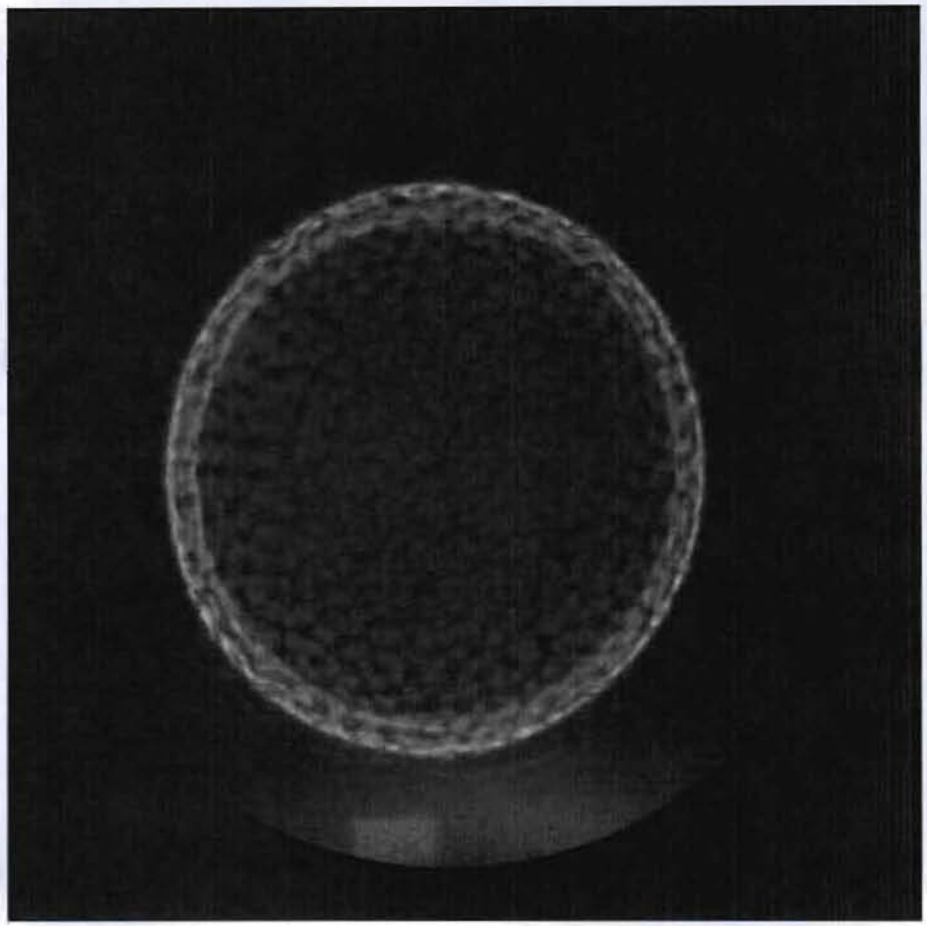

Fragments Can be Recovered through "Soft Catch"

L. Hull

Shear Localization and Breakup

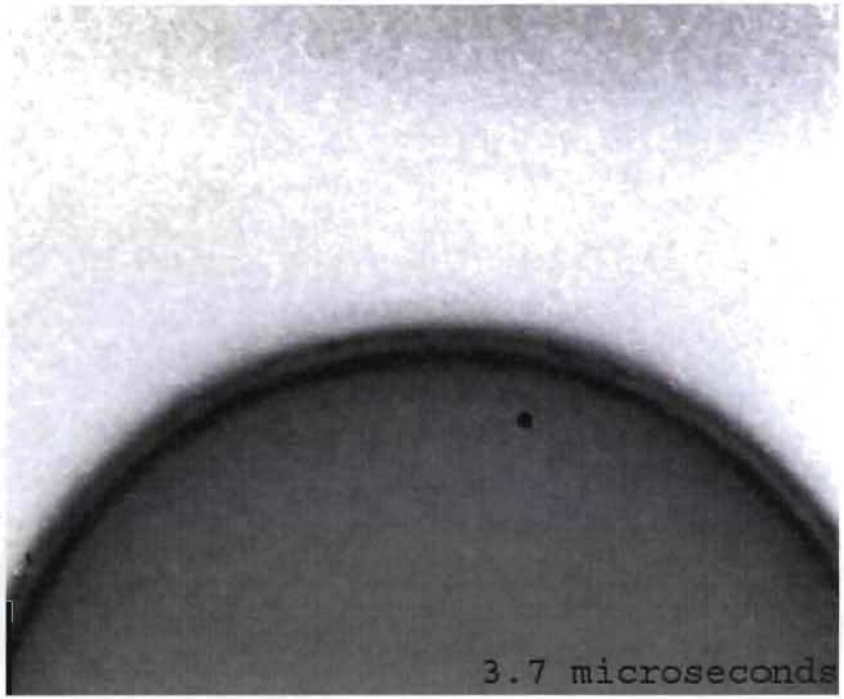

Frame 0:	0 μs	pre-Shot Static
Frame 1:	3.7 μs	hint of localization
Frame 2:	5.9 μs	clear localized thinning
Frame 3:	7.0 μs	continued thinning
Frame 4:	8.0 μs	localization points begin to connect
Frame 5:	11.4 μs	continued fragmentation
Frame 6:	14.6 μs	fragments formed
Frame 7:	16.8 μs	ballistic motion

Shear Band Failure in U6Nb

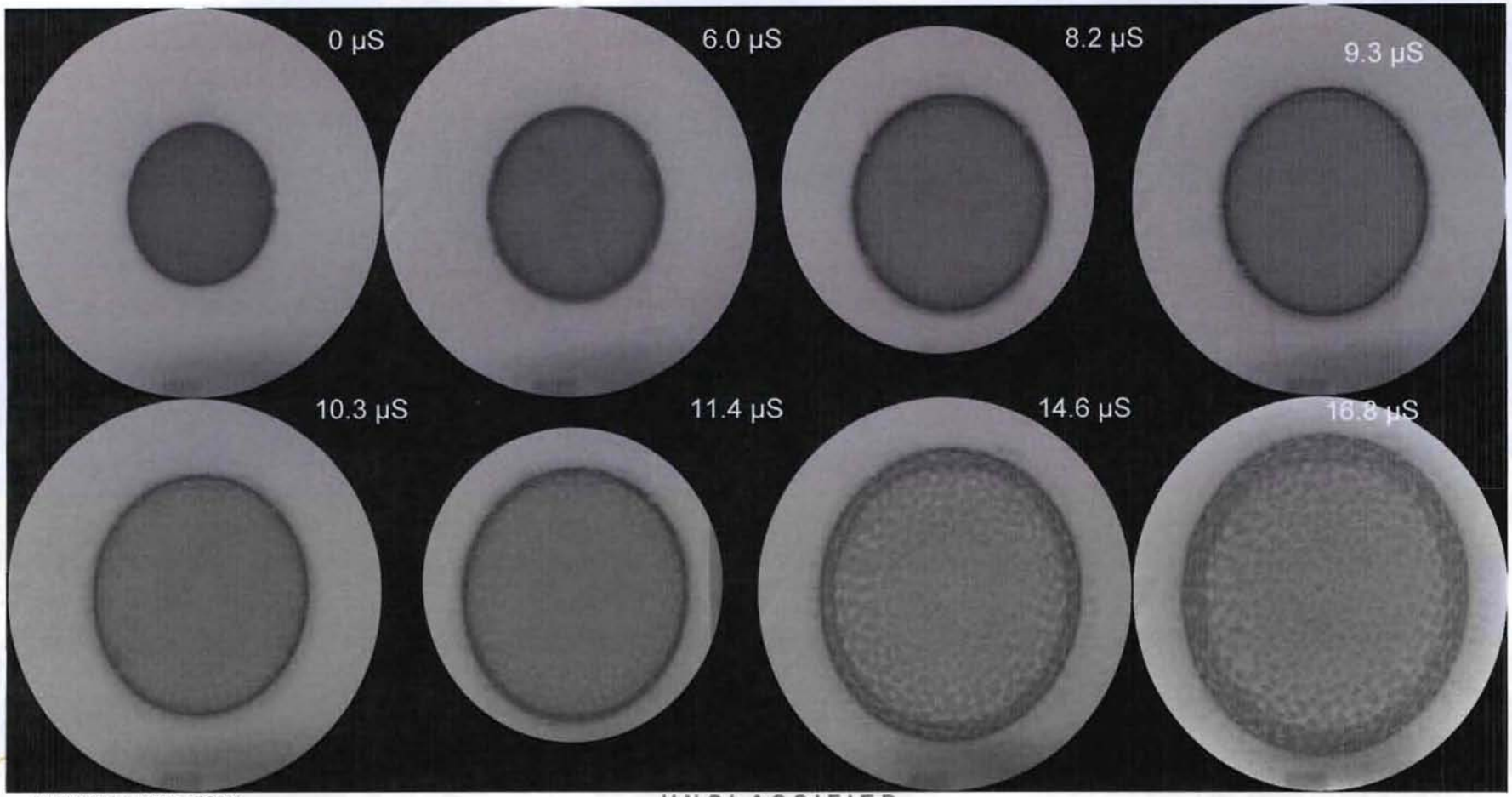

Shear Band Failure in U6Nb

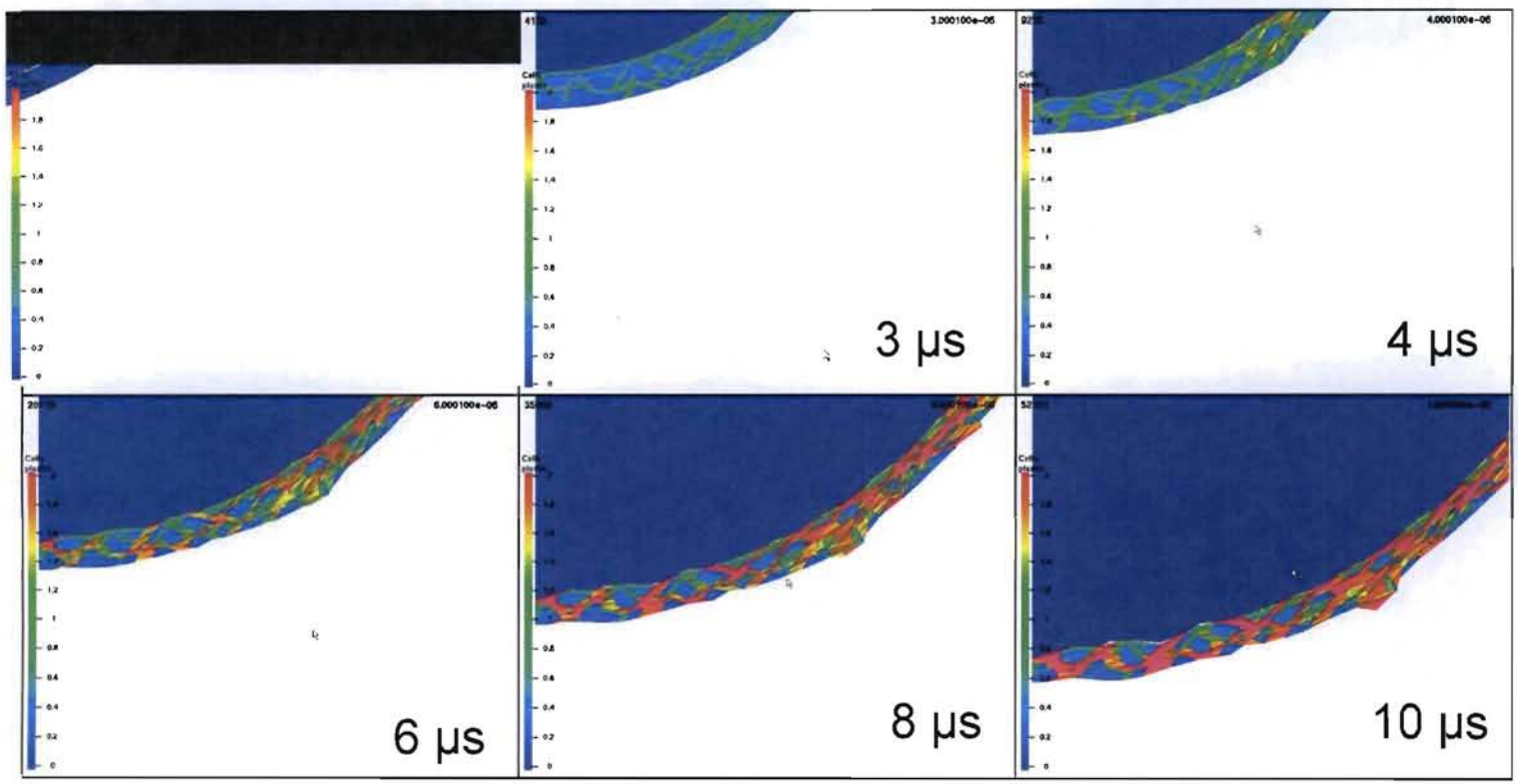

We Estimate Percent Open Area from 100 Random Locations

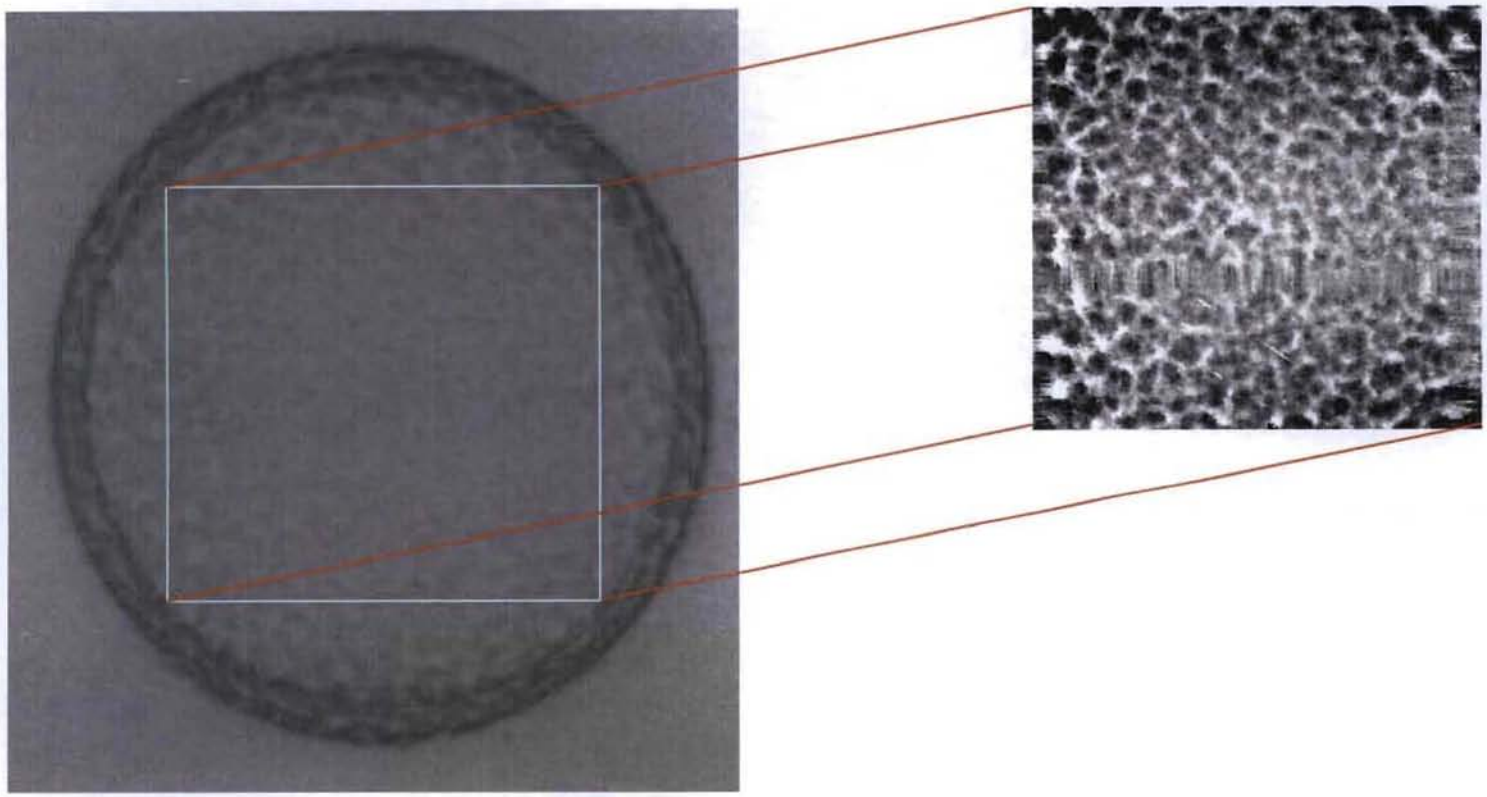

10mnstfprad0161Shot2.tif

- 100 random points are thrown at the data set
- Metal/Not-metal determined at each point by eye
- Tedious, but very effective

Los Alamos
NATIONAL LABORATORY
EST. 1943
Operated by the Los Alamos National Security, LLC for the DOE/NNSA
NNSA

This Procedure is Repeated over Four pRad Time Steps by 15 Individuals

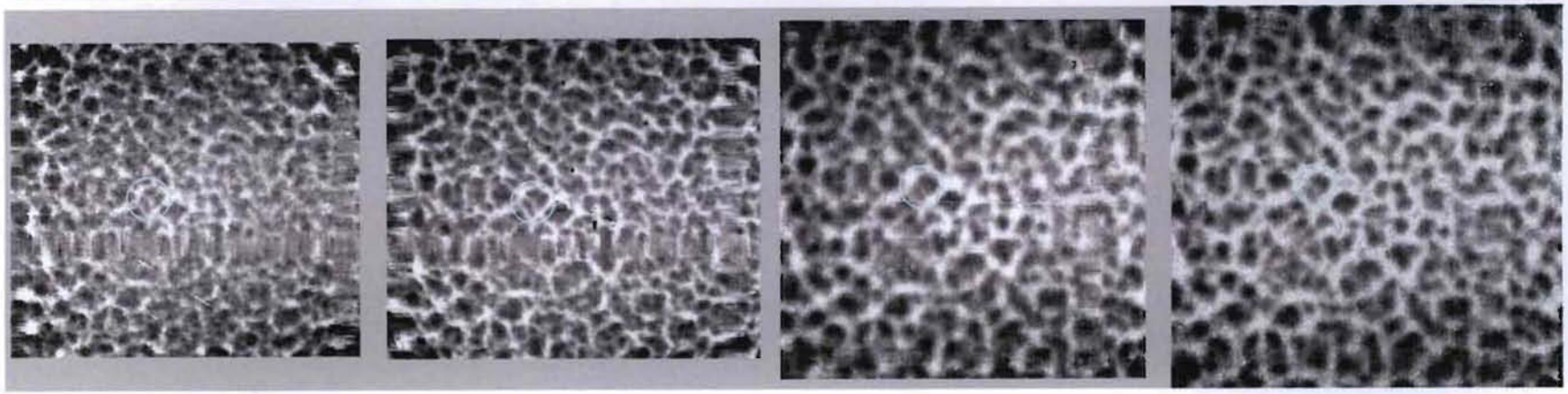

15.7μs 26% open | 17.8μs 34% open | 20.0μs 39% open | 22.1μs 51% open

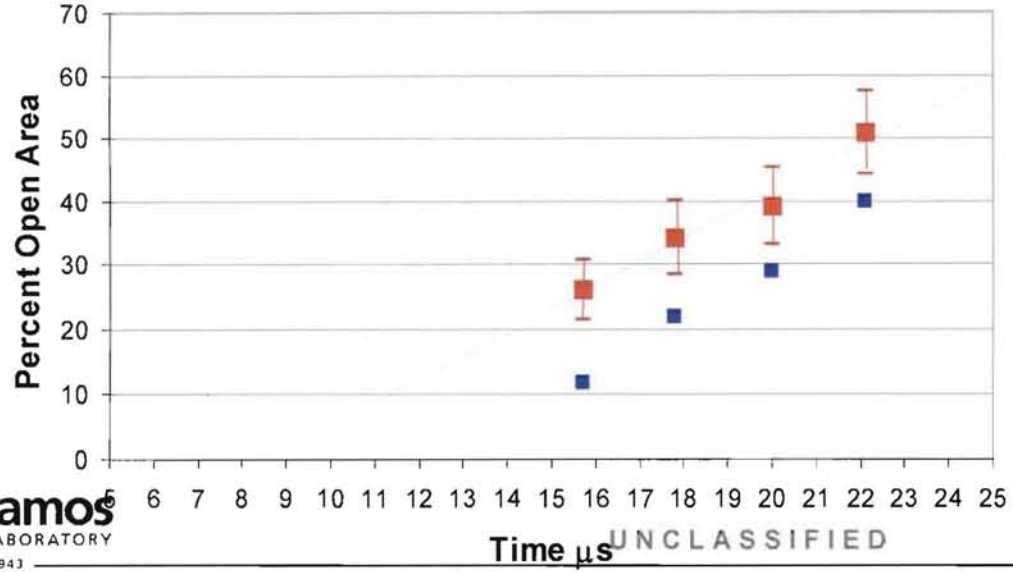

Shear Band Failure in U6Nb

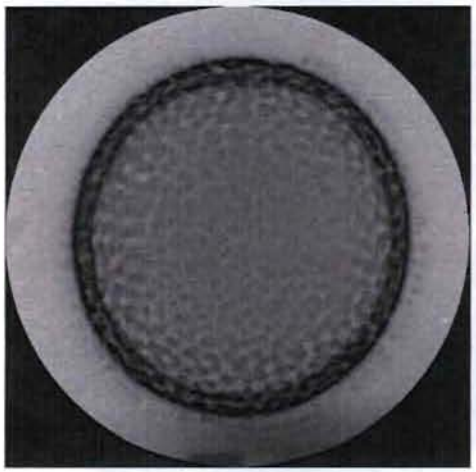

- Assume no HE products to give max DU density.
- Assume flat measured HE products to calculate min DU density.
- Results bracket density in cracks.

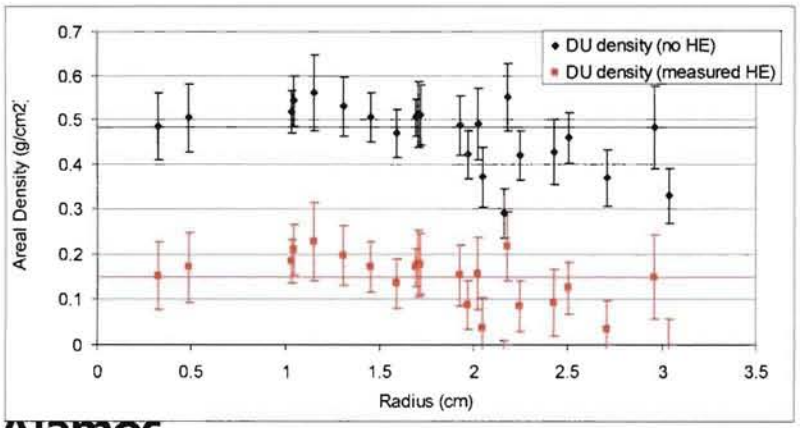

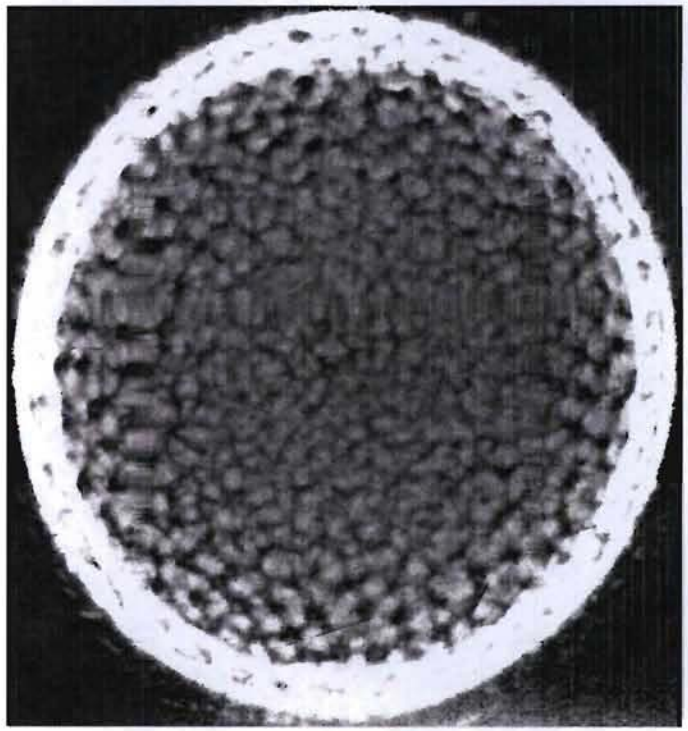

pRad has been used to make a movie of the development of a Richtmyer-Meshkov (RM) instability in solid tin (W. Buttler)

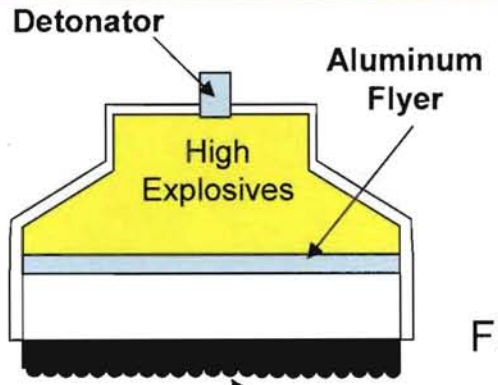

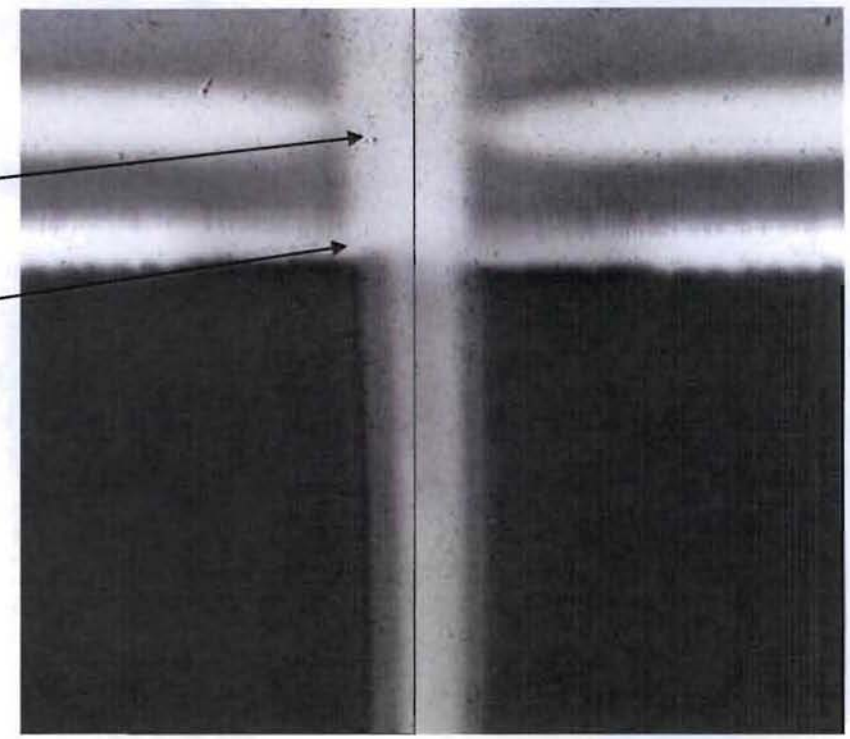

The target has a sin wave machined in its lower face

Richtmyer-Meshkov with uniform perturbation (RM) instability in molten tin

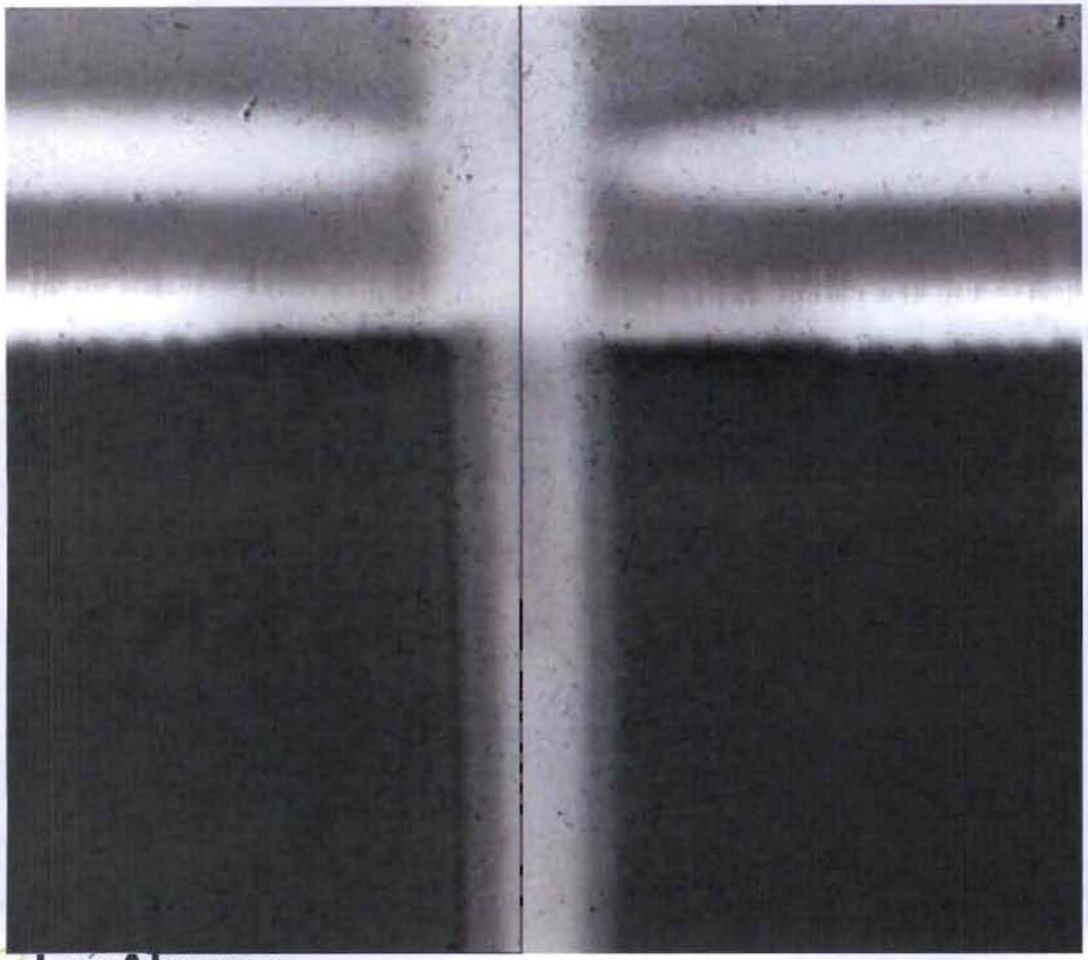

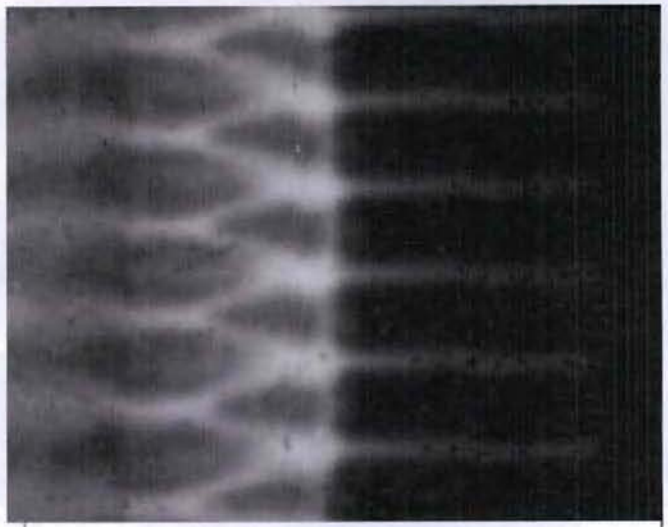

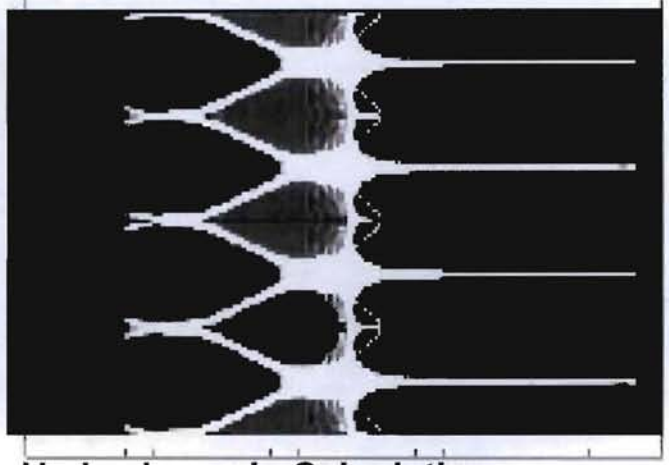

Hydrodynamic Calculations
(David Youngs et al.)

More RMI experiments: A group of three perturbations

vacuum | 5 atm, of Xe | 5 atm, of Ne

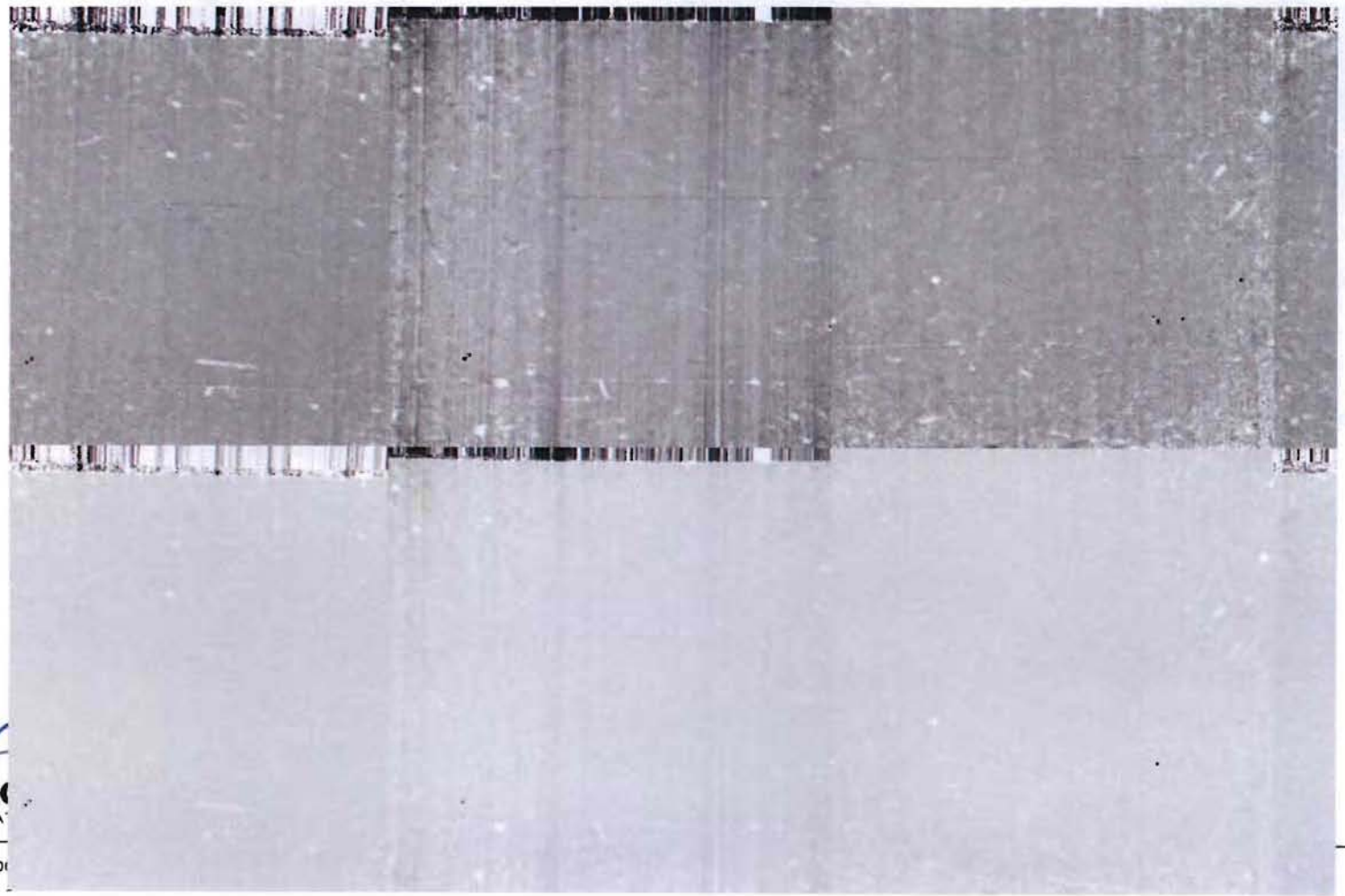

Material Strength Experiments
R. Olson

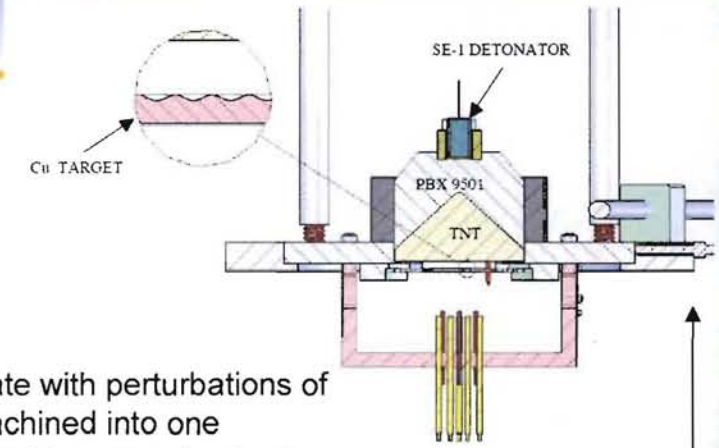

The technique utilizes a flat metal plate with perturbations of known wavelength and amplitude machined into one side of the plate. High explosive is used to generate shock-free, planar loading on the perturbed side of the plate and the amplitude of the Rayleigh-Taylor (R-T) unstable perturbations are measured from radiographs acquired as a function of time (see Fig. 1). The perturbation growth rate is directly related to the dynamic shear strength of the metal and thus can be compared directly to that predicted by various strength models via hydrodynamic calculations.

- Utilized improved resolution capability of new magnifier system.
- Six (or more) dynamic experiments performed to study instability growth versus drive pressure by varying HE standoff.
- Demonstrated shockless acceleration and reproducibility.

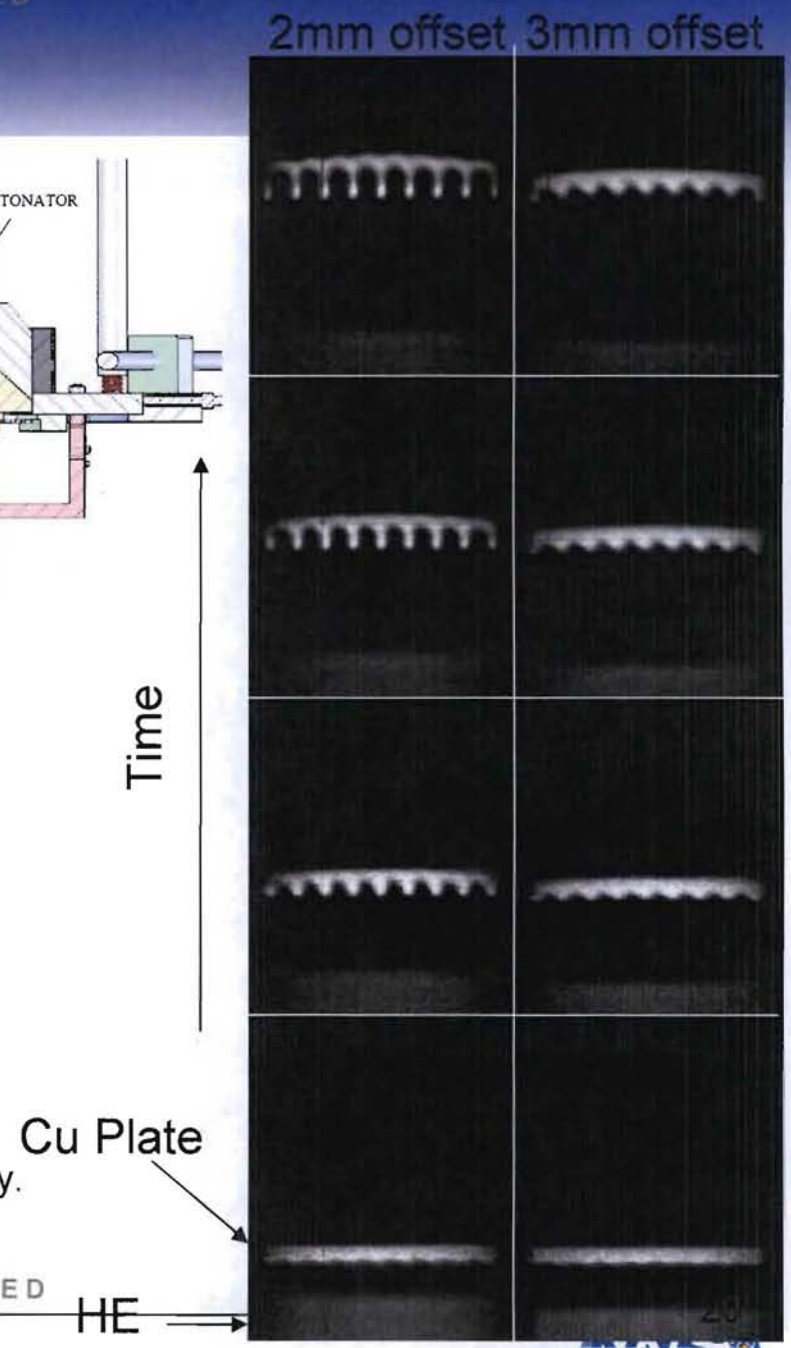

Investigation of Dynamic Phase Transitions in Metals using the 40mm Launcher in Area C

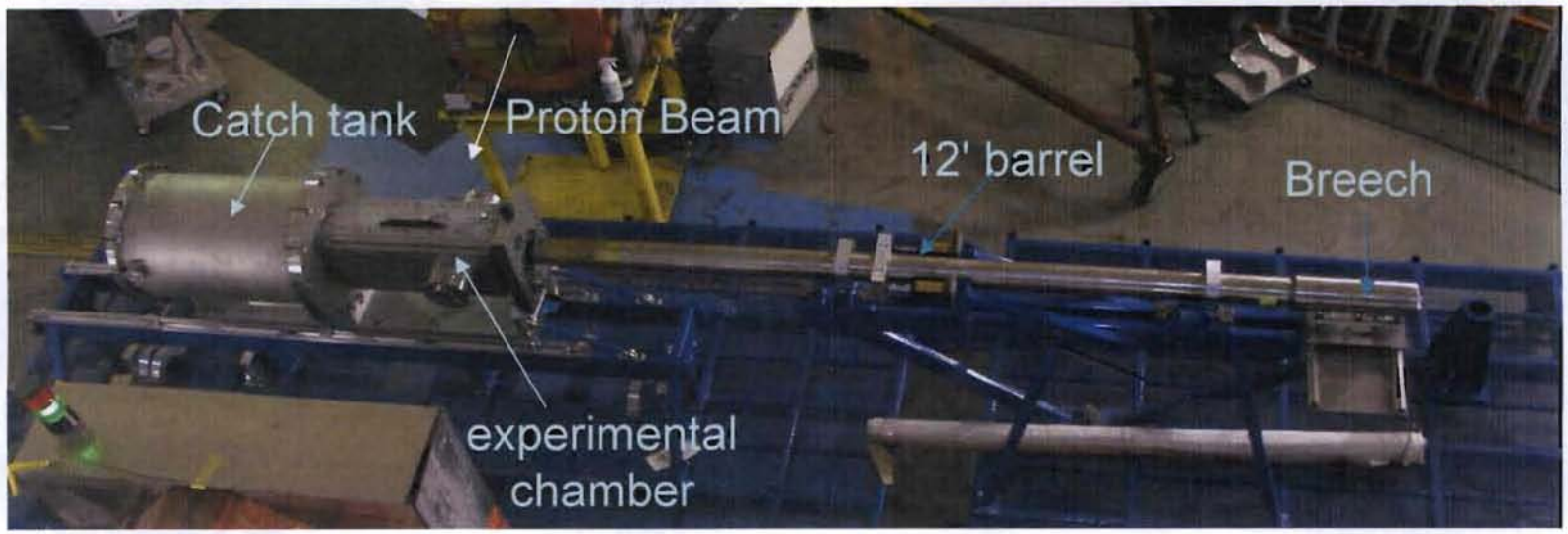

P. A. Rigg, C. L. Schwartz, F. J. Cherne, G. T. Gray III

Powder Gun Coupled with pRad

- 1-2 mm/μs projectile
- Planar drive
- Synchronized to proton pulses
- Supported shock wave

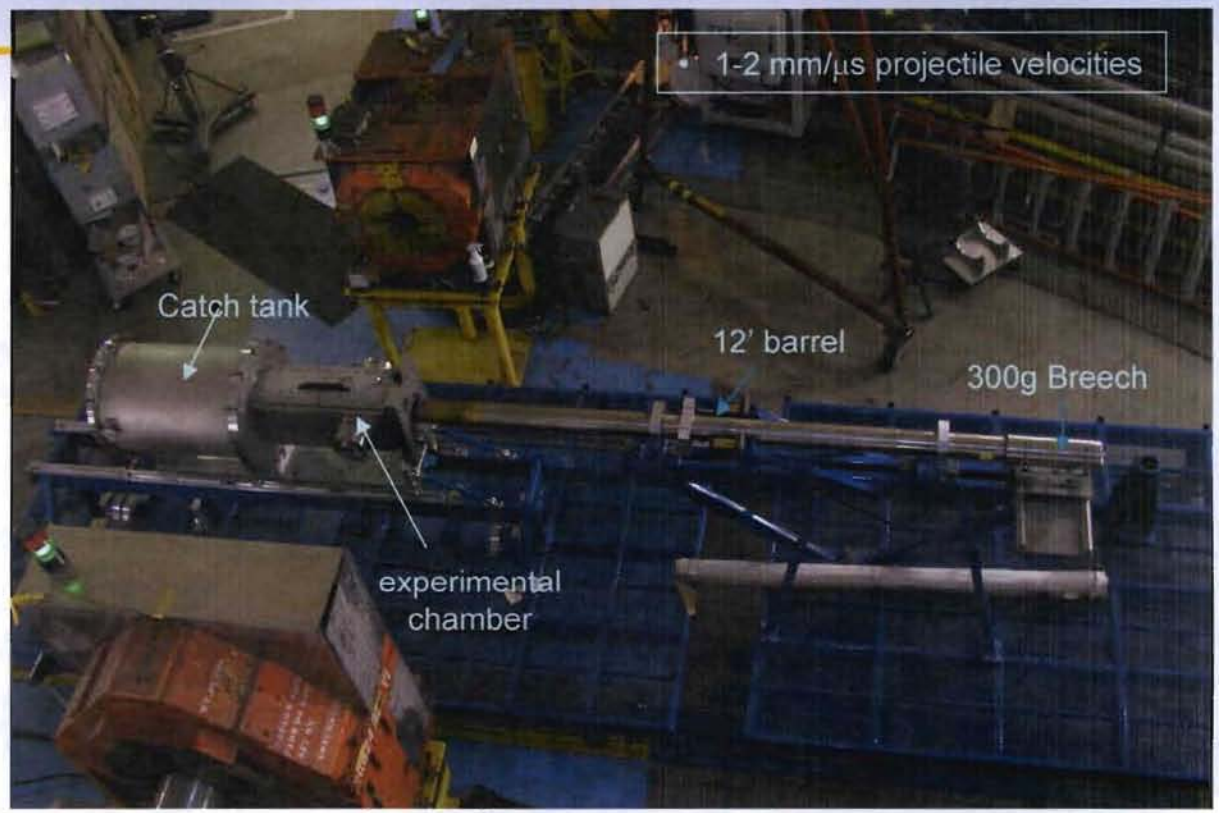

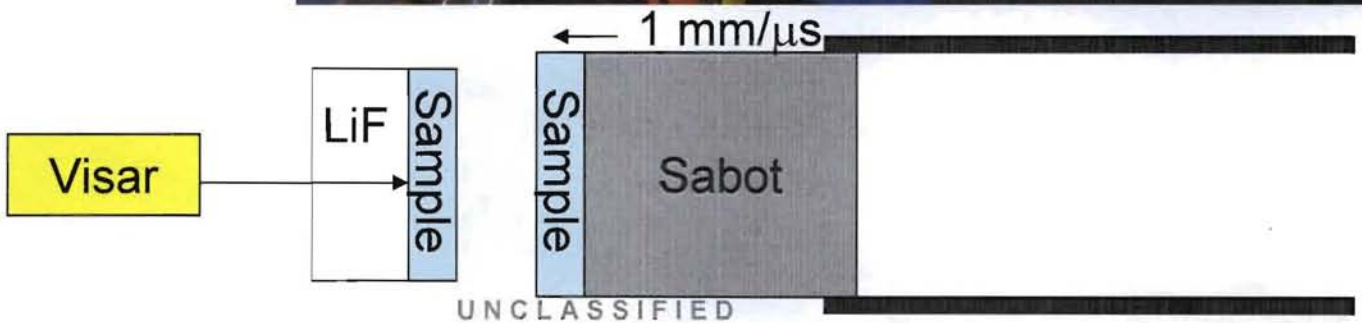

40mm Launcher Design Details

- Completely enclosed system designed to couple plate impact experiments with Proton Radiography
- Uses gun powder and an SE-1 detonator to launch projectiles up to 2 km/s (600 kbar in copper using Ta flyer)
- Produces planar impact on samples up to 40mm in diameter
- Free floating barrel design and shock absorber system minimize recoil load transferred to Proton beam tubes

Synchronization

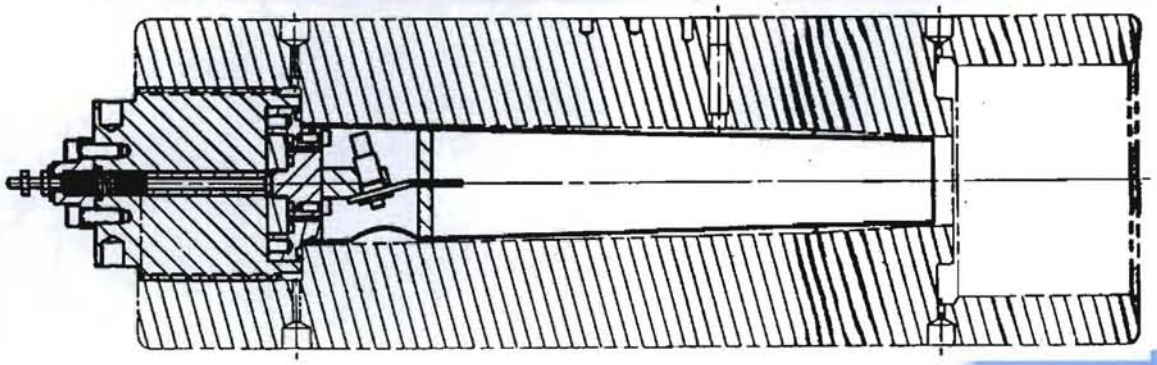

Det fired system:
Beamline initiates gun

Use of shear disk
greatly reduces jitter

Motivation

- Density measurements with 0.5% to 2% accuracy needed to develop accurate equations of state
- Direct density measurement techniques and data are lacking
  - Calculated values can have unacceptably large error
  - Quantitative Dynamic X-Ray Diffraction data currently limited to single crystals
  - X-Ray radiography limited to a few snapshots per experiment
- Plate impact technique provides well-characterized 1-D shock loading to samples
- PRAD can provide both direct density measurements and resolution of mesoscale feature with many frames of data per experiment
- Can coupling provide quantitative, real-time measurements of meso-scale processes for the first time? Can accurate density measurements behind shock front be achieved?

Density Measurements in Aluminum and Copper

- Four symmetric impact experiments were completed
  - Two experiments on 6061-T6 Aluminum
  - Two experiment on OFHC Copper
  - All samples backed by LiF window to maintain stress at back

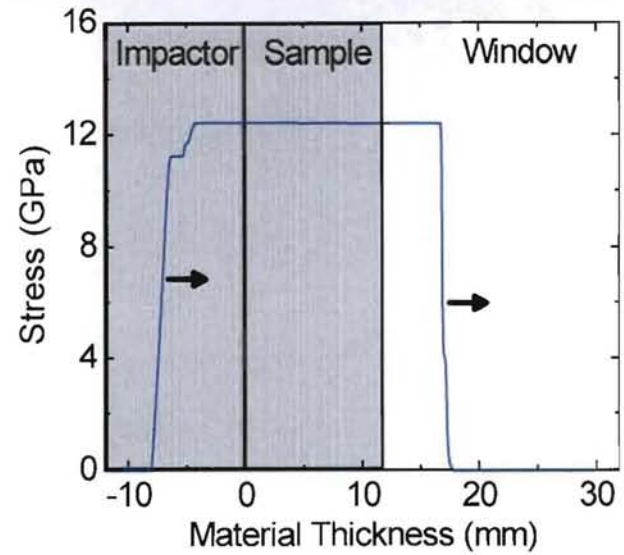

- High confidence in EOS for Aluminum and Copper
- Calculate density using Jump Conditions given $P(u_P)$ and measured projectile velocity, u_0

$$u_P = \frac{1}{2}u_0 \qquad P = \rho_0 U_S u_P \qquad \rho = \frac{\rho_0 U_S}{U_S - u_P}$$

- Measure u_P at Sample/Window interface as check

Radiography Results – Aluminum Symmetric Impact

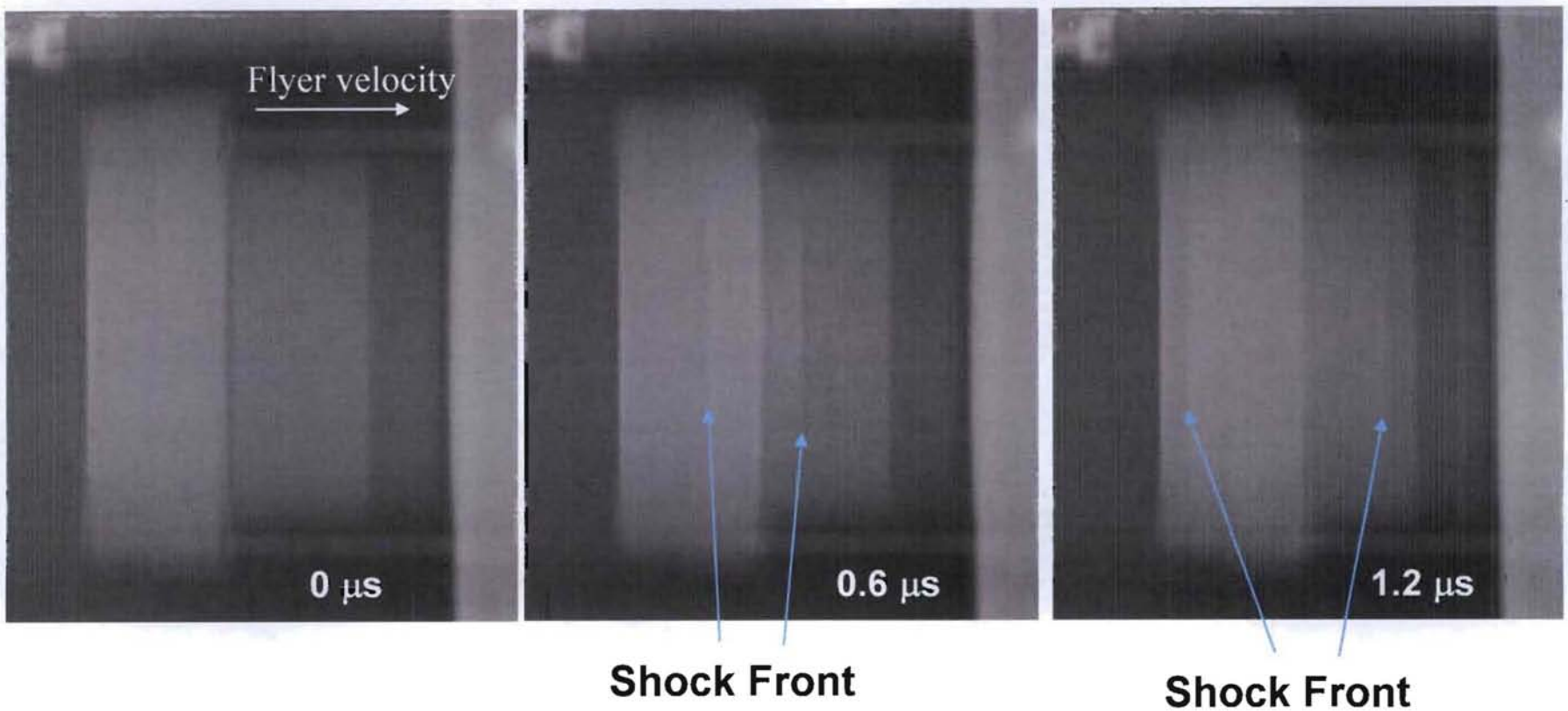

Radiography Results – Aluminum Symmetric Impact

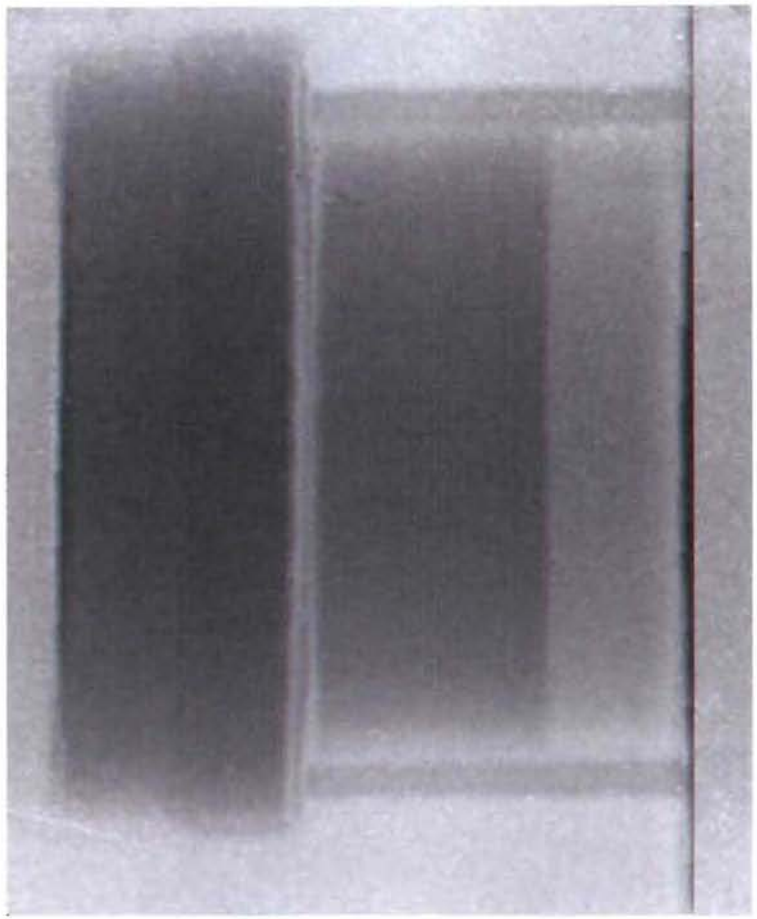

Density Calculation – Jump Conditions

Impact Velocity

$u_0 = 1.452 \pm 0.012$ mm/μs

Particle Velocity: ½ u_0

$u_P = 0.726 \pm 0.006$ mm/μs

$P(u_P)$ for 6061-T6 Al

$P = 1.184 + 140.2u_P + 37.38u_P^2$

$P = 12.27 \pm 0.09$ GPa

Initial density from immersion

$\rho_0 = 2.710 \pm 0.003$ g/cm^2

VISAR Record for Shot prad 0198

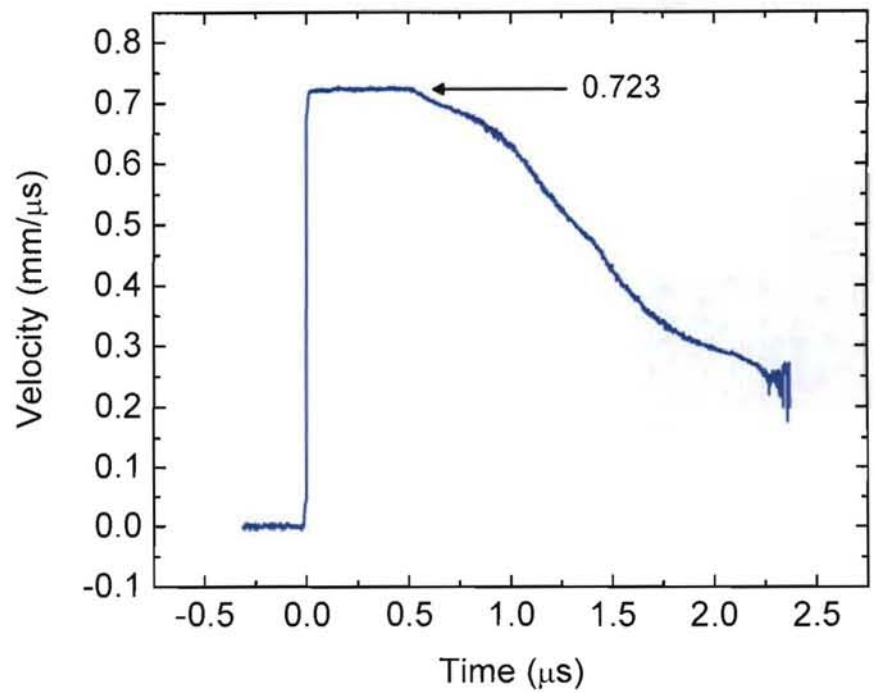

Calculate density from Jump Conditions

$$\rho = \frac{\rho_0 P}{P - \rho_0 u_P^{\,2}} \quad \Rightarrow \quad \rho = 3.067 \pm 0.009 \text{ g/cm}^3 \quad (0.3\%)$$

Density Calculation – Abel Corrected Radiograph

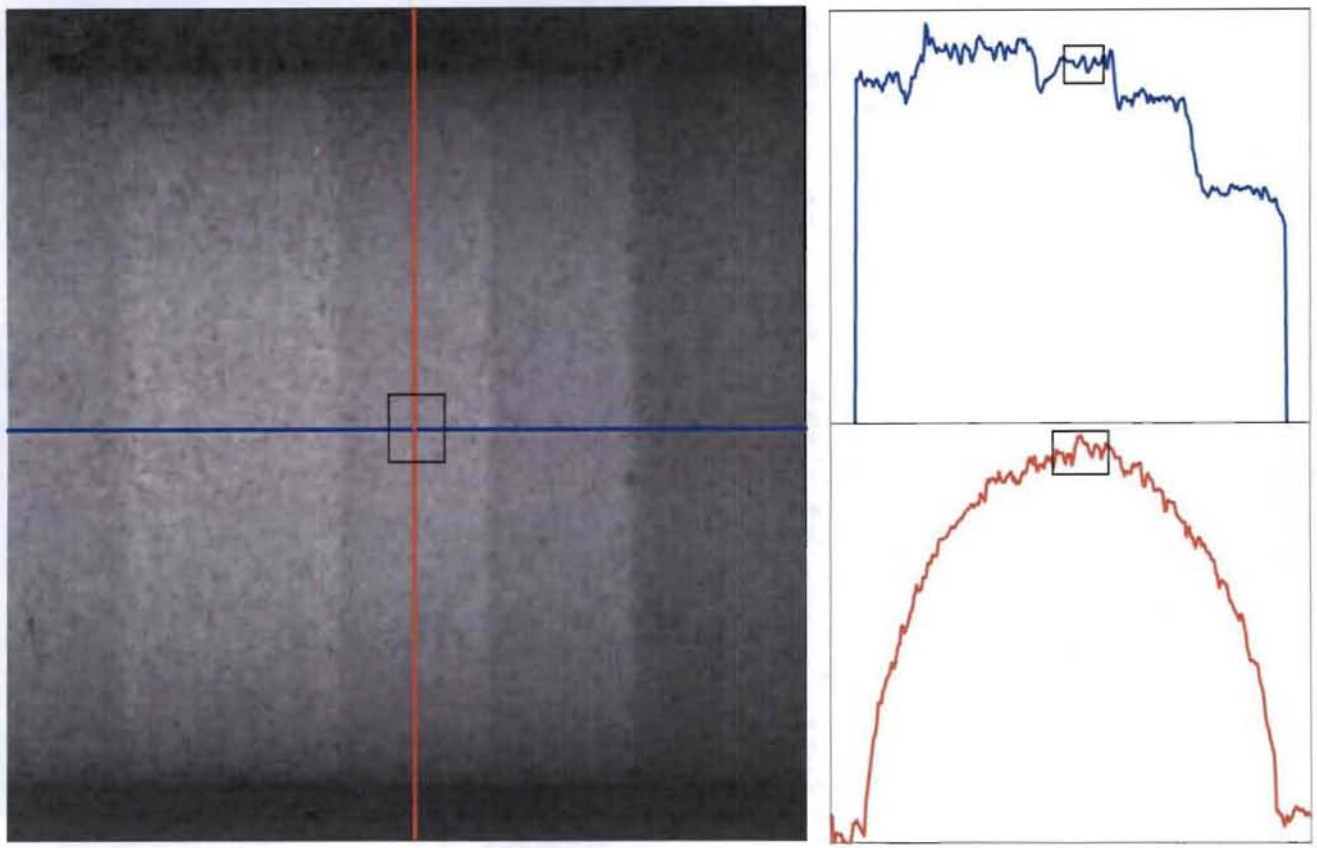

Density: $\rho = 3.07 \pm 0.03$ g/cm^3 (1.1%)

Demonstration Powder Gun Experiment

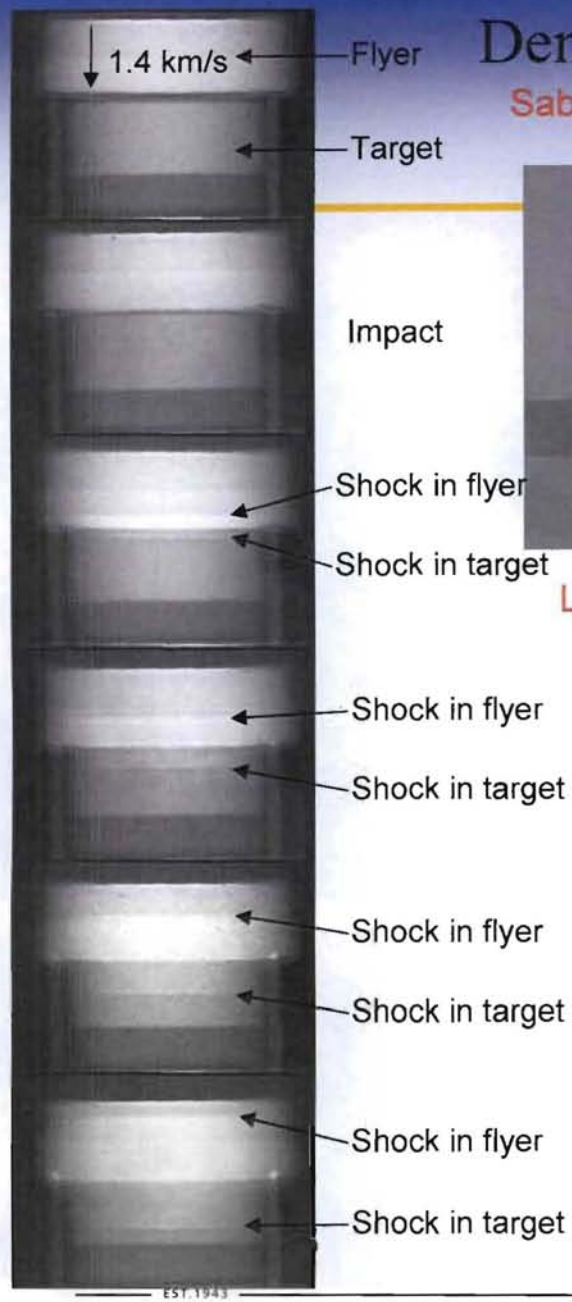

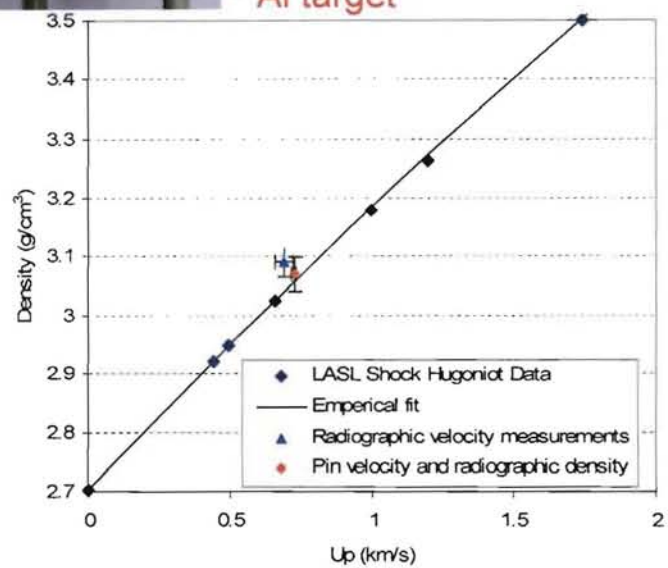

Two methods of measuring a point on shock Hugoniot per dynamic event:

- Radiographic measurement of density behind shock front.
- Simultaneous measurement of particle and shock velocity

Invited Talk : Paulo Rigg, *Shock Compression of Condensed Matter*, 2007

Rigg, Schwartz, et al., *Phys. Rev. B*, Jun 08, vol. 77, iss. 22 220101

EST. 1943
Operated by the Los Alamos National Security, LLC for the DOE/NNSA

Density Calculation – Radiographs

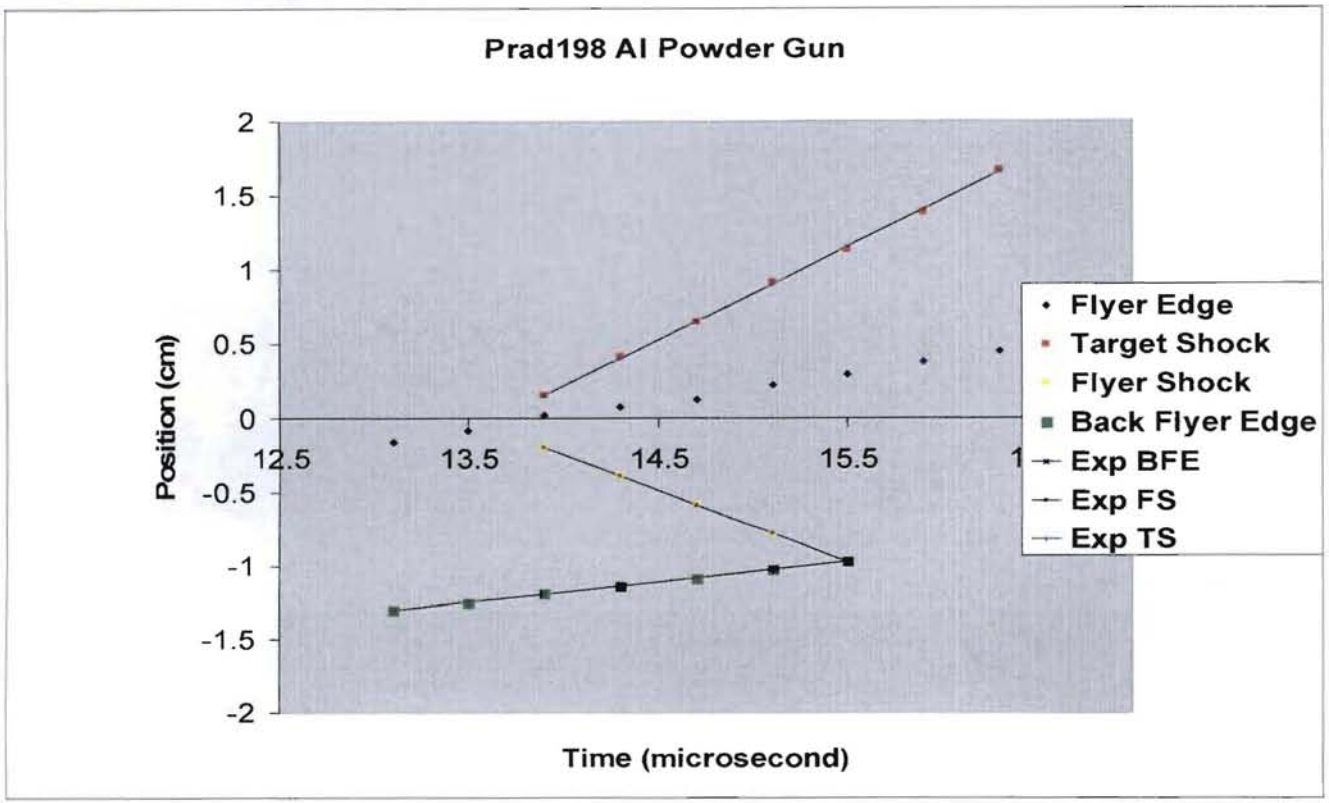

f. Shock: $x_0+(u_p-u_s)(t-t_0)$

t. Shock: $x_0+(u_p+us)(t-t_0)$

f. BEdge: $x_0+2u_p(t-t_0)-d$

$u_p = .692 \pm 0.06$ mm/μsec

$u_s = 6.27 \pm 0.04$ mm/μsec

Density: $\rho = 3.04 \pm 0.024$ g/cm3

Ex Density : $\rho = 3.067 \pm 0.009$ g/cm3

Results from Copper Symmetric Impact Experiment

Flyer velocity →

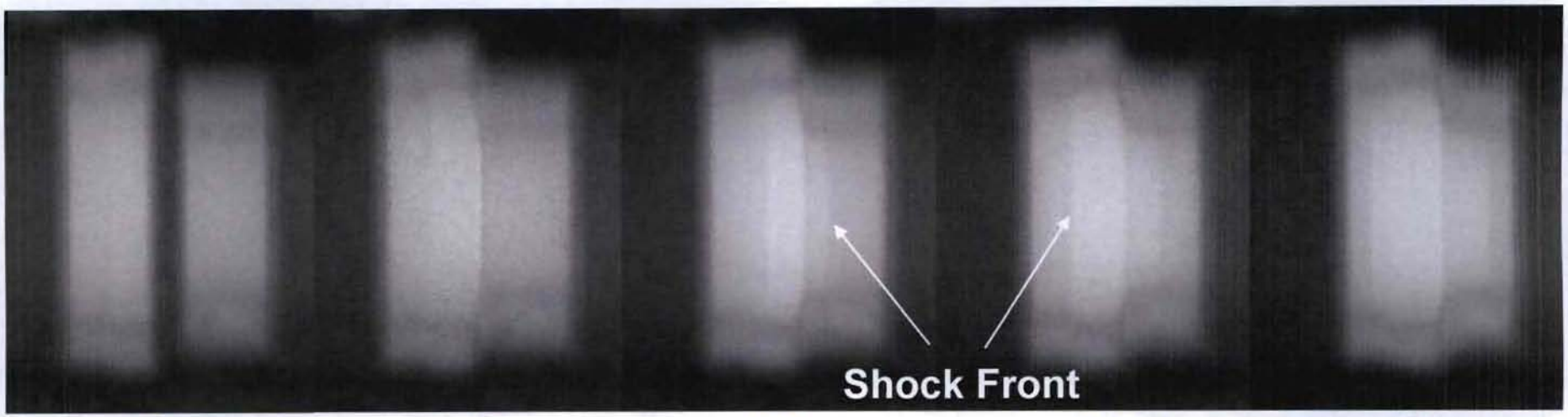

-1.54μs 0 .57μs 0.86μs 1.26μs 1.66μs

- Significant distortion present due to higher density of copper
- Distortions do not affect measurement

Experiment Summary

Experiment	Impactor/ Sample	Impactor Velocity (km/s)	Peak Stress (GPa)	Initial Density (g/cm^3)	Calculated Density (g/cm^3)	Measured Density (g/cm^3)	Agreement
1	Al 6061-T6	1.452 (0.012)	12.27 (0.11)	2.710 (0.003)	3.067 (0.005)	3.07 (0.03)	0.1%
2	Al 6061-T6	1.422 (0.002)	11.98 (0.03)	2.710 (0.003)	3.060 (0.004)	3.056 (0.03)	0.1%
3	OFHC Cu	1.30 (0.04)	28.59 (0.91)	8.928 (0.003)	10.30 (0.05)	10.28 (0.10)	0.2%
4	OFHC Cu	1.249 (0.002)	27.16 (0.06)	8.928 (0.003)	10.241 (0.006)	10.28 (0.10)	0.4%

- Agreement between measured and calculated values better than 0.5% for all experiments

Measured Density Values Lie on Hugoniots

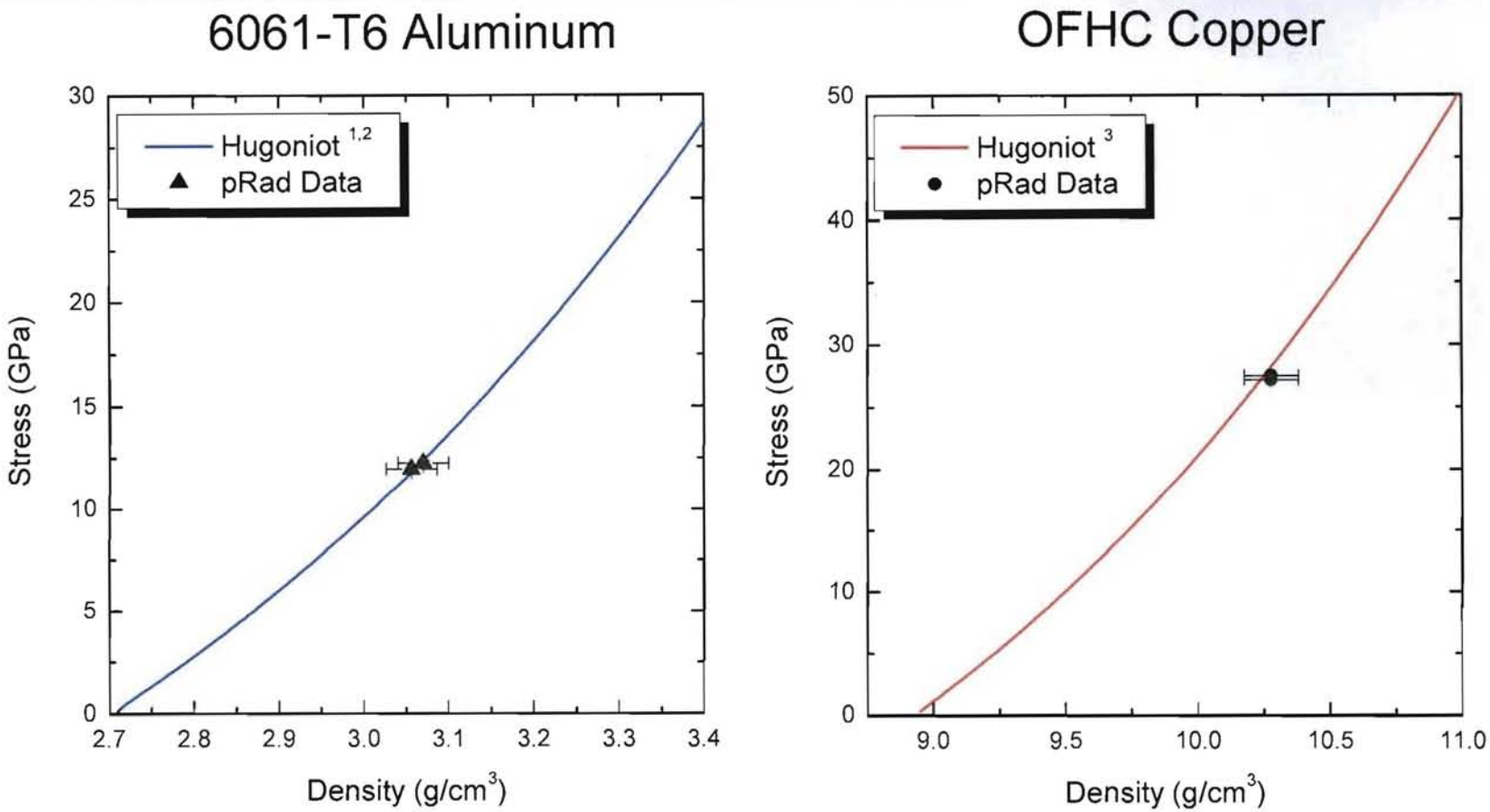

(1) C. D. Lundergan and W. Herrmann, J. Appl. Phys. **34**, 2046 (1963).
(2) W. M. Isbell and D. R. Christman, Tech. Rep. MSL-69-60, General Motors (1970).
(3) R. G. McQueen, S. P. Marsh, J. W. Tayor, et. al., *High Velocity Impact Phenomena* (Academic Press, New York, 1970).

Phase Transition Studies: Iron

- α to ε transition observed in Fe at ~13 GPa
- Transition is relatively insensitive to purity
- Reverse transition clearly observed as evidence by rarefaction shock

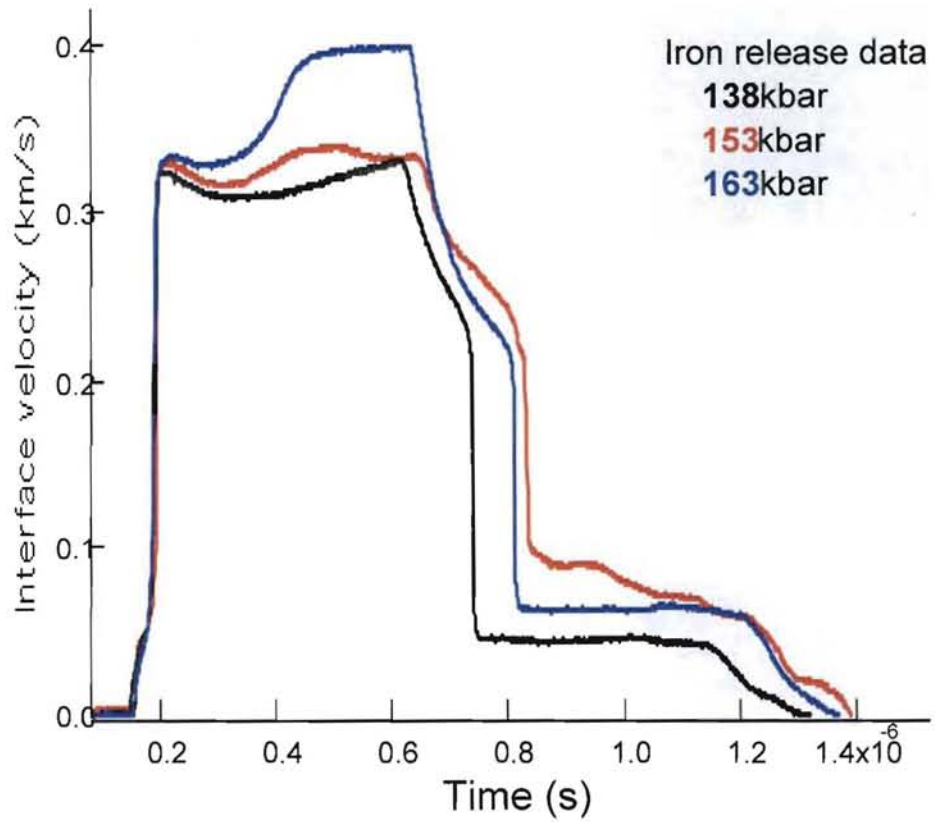

Two-wave structure observed in Iron

- Aluminum impacting Iron backed by Sapphire @ 1.45 km/s -> 175 kbar in Fe
- 3X pRad Magnifier used to enhance contrast and sharpness

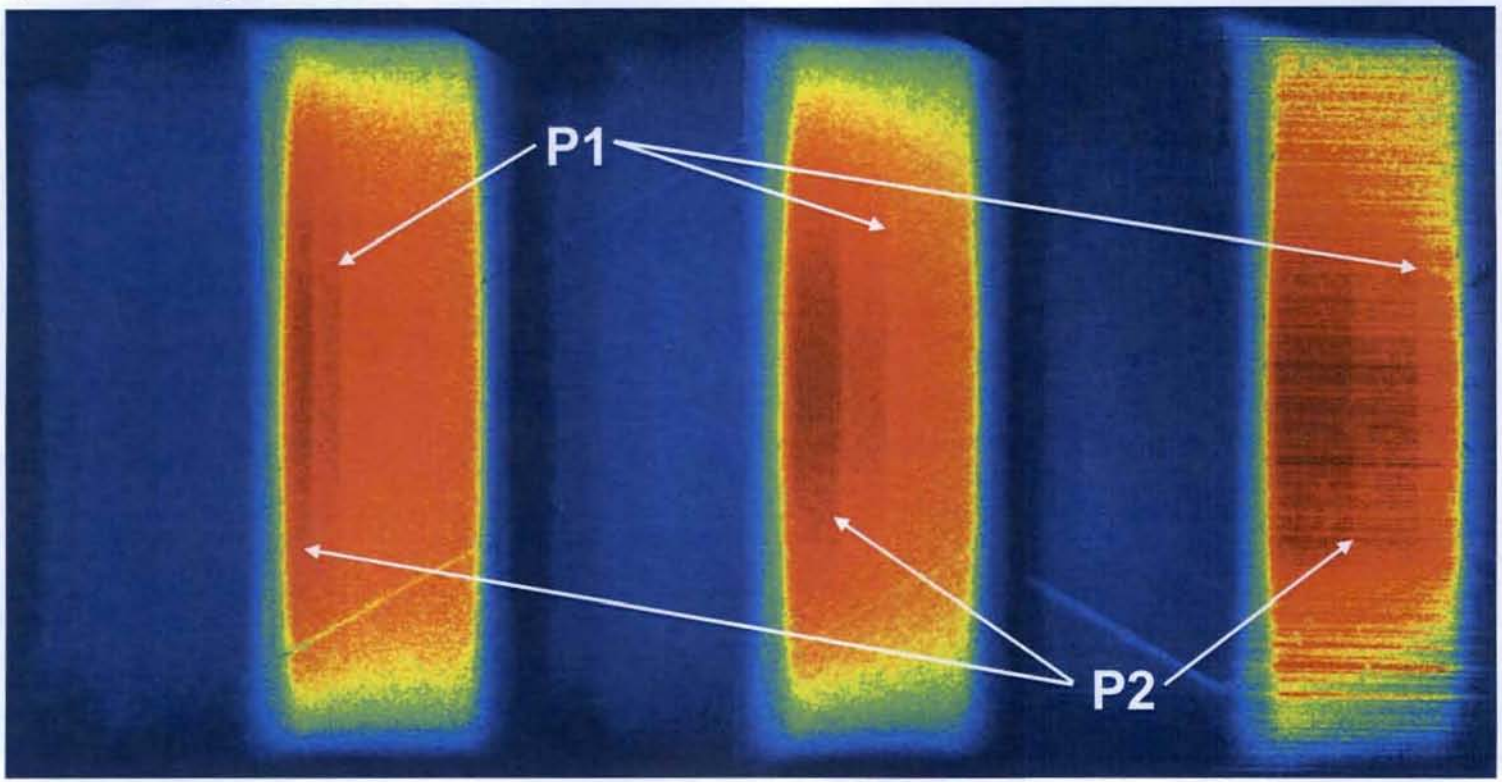

Measured and Calculated Densities - Iron

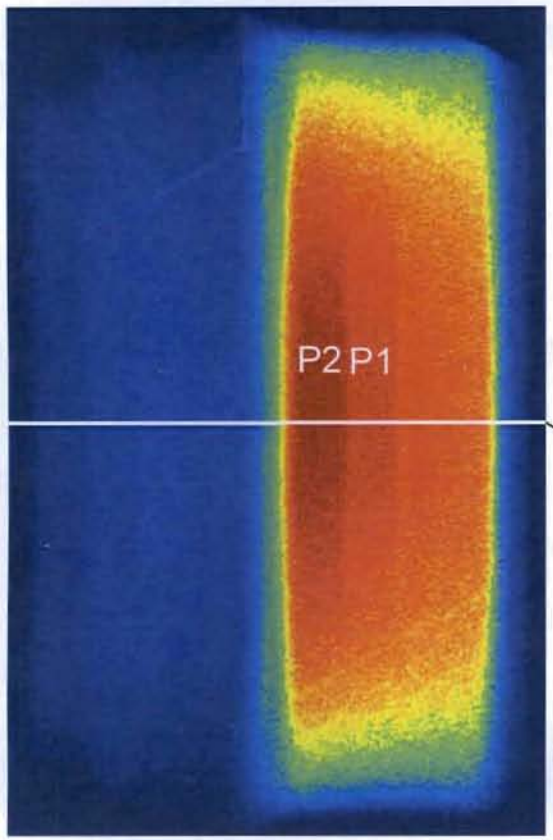

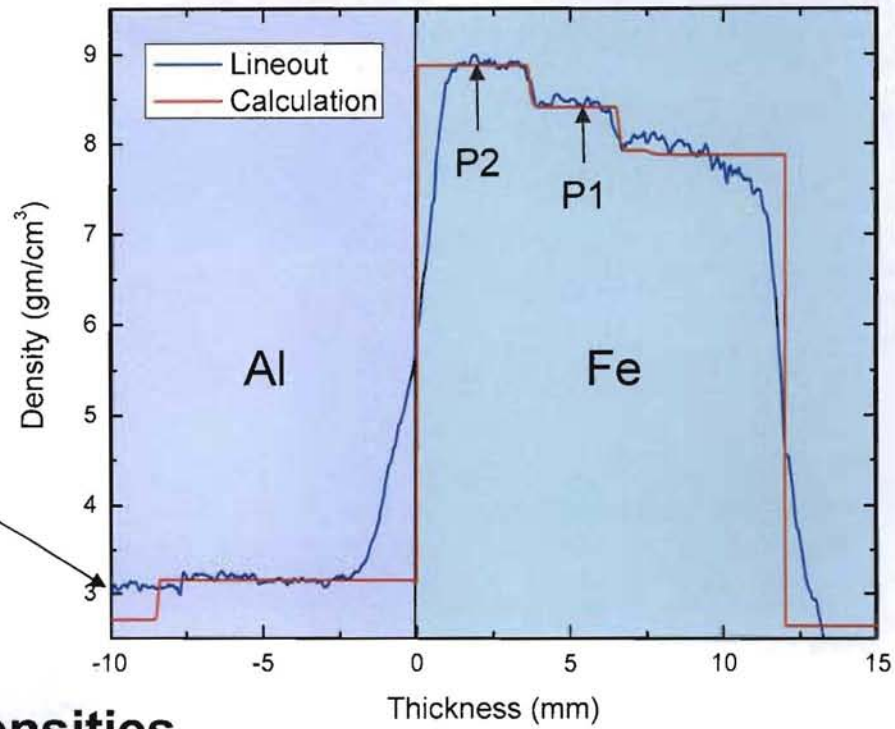

Densities

State	Measure	Calculat	Agreem
P1	8.346	8.342	<0.1%
P2	8.854	8.846	0.1%

Results

- Successfully coupled proton radiography with plate impact experiments
- Direct density measurements obtained in shocked aluminum, copper and iron with ~1% precision
- Agreement with calculated values better than 0.5%!
- Large difference in initial density between Cu and Al shows wide applicability to other materials
- Future work: Cerium to examine solid-solid and solid-liquid phase transitions…

Taylor Wave-Driven Tin

- Explosive-driven "Taylor Wave" shock
- Multiple pressures, decaying over time
- Stainless steel membrane

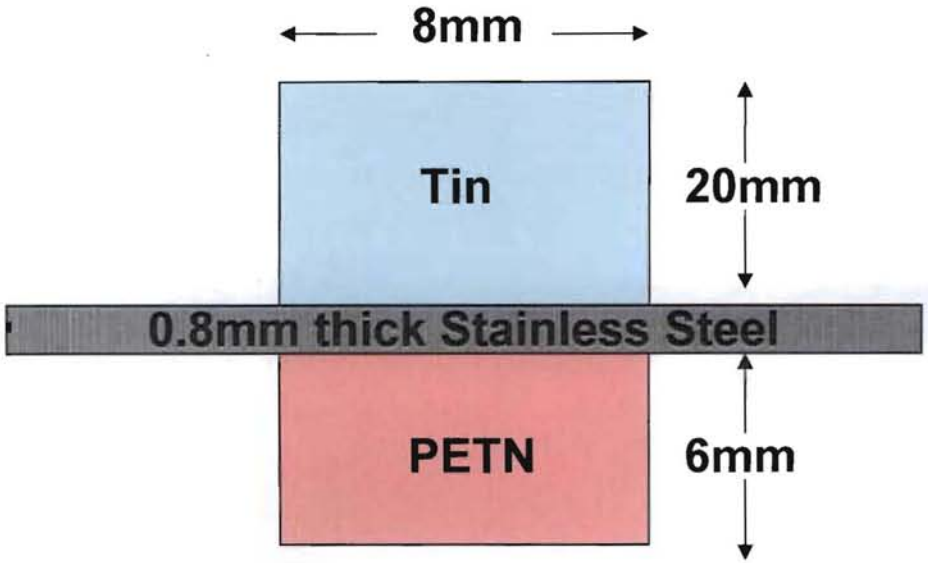

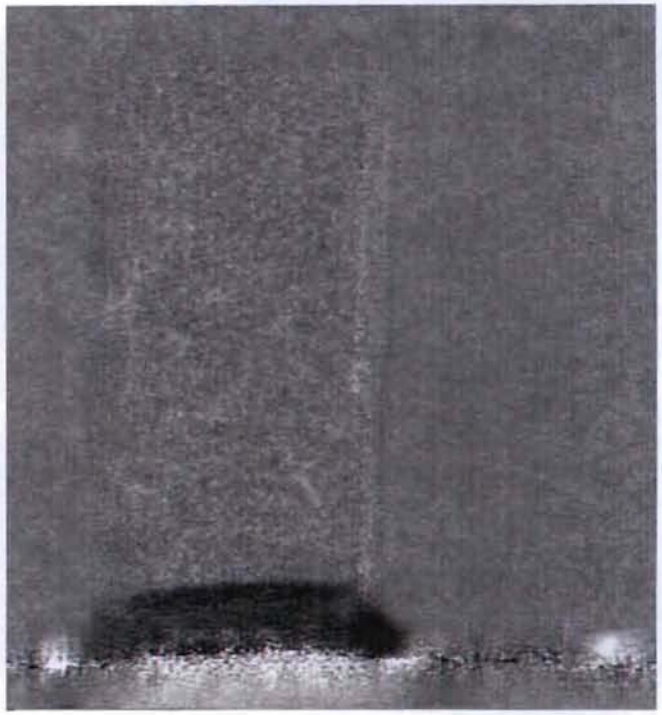

Dynamic / Static transmission radiographs

Rusty Gray provided "pristine" tin sample

Tomographic reconstruction and subtraction of overburden

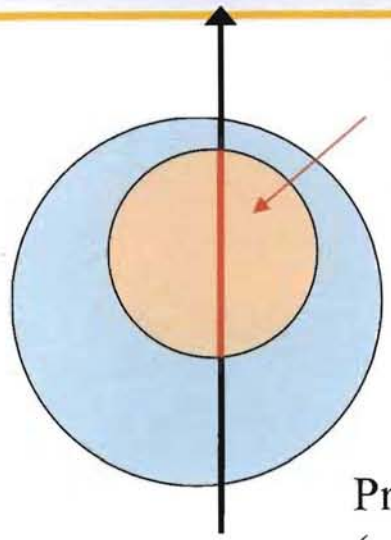

Experiment

Overburden

Tomographic Reconstruction (Abel Inversion)

Converts line integrals to volume density map

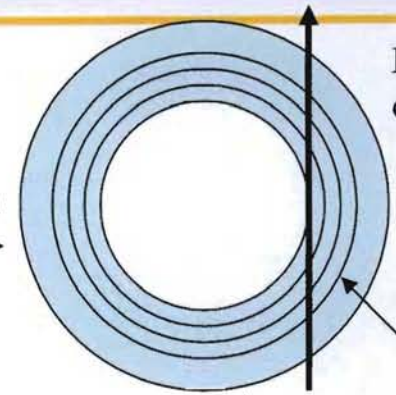

Proton path thru overburden

Reconstructed density map

Projection: converts density map back to line integrals

Proton path
(red is the good part;
We'd like to subtract the black)

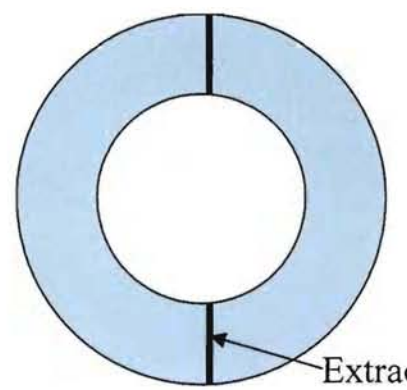

Extracted and projected line integral through overburden

Subtraction

Leaves only the data we want

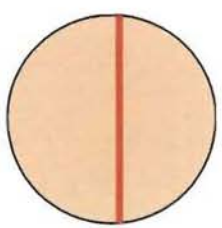

Trimmed density reconstruction

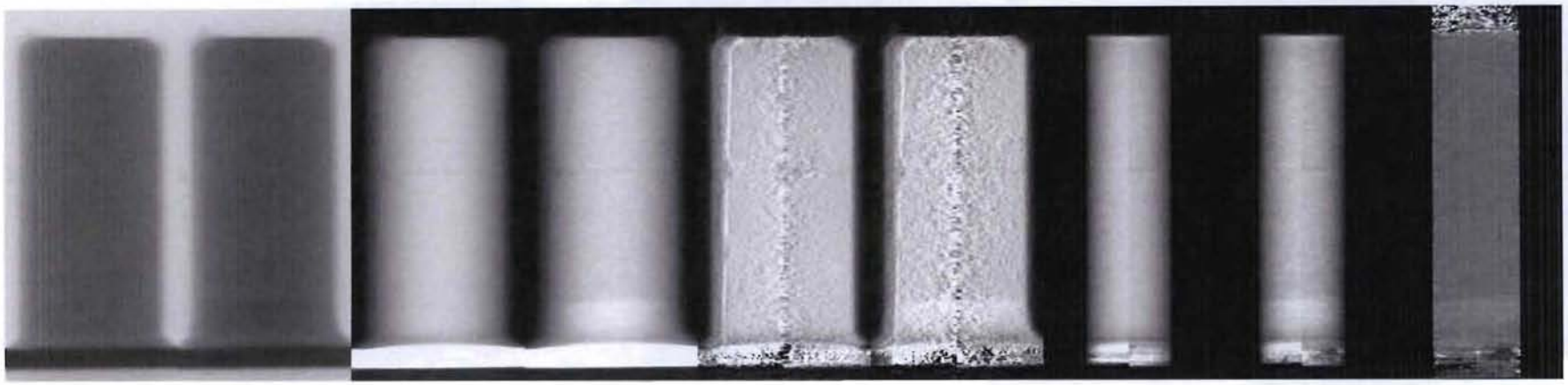

Technique that subtracts overburden and release effects from areal density radiographs

Position and Density Measurements

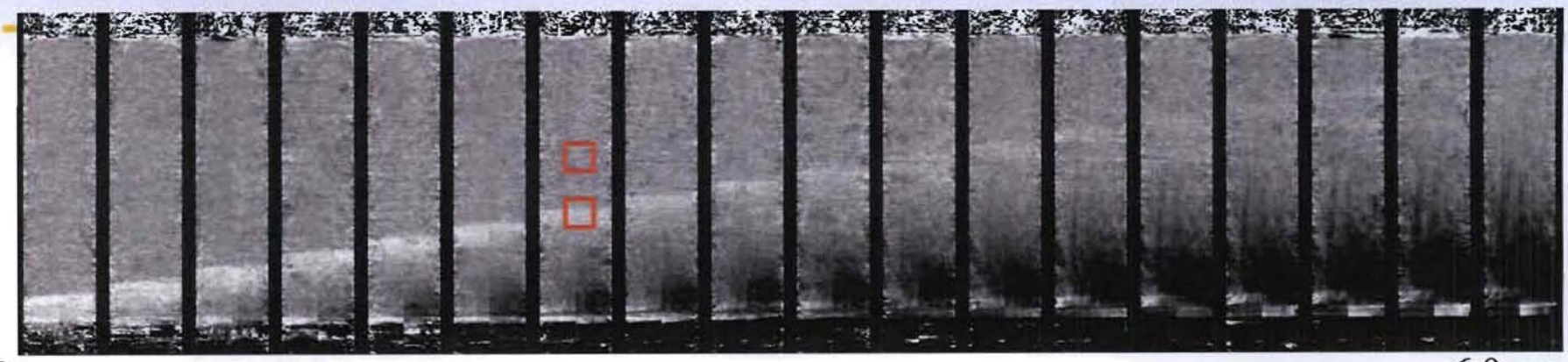

1.8μsec Time 6.9μsec

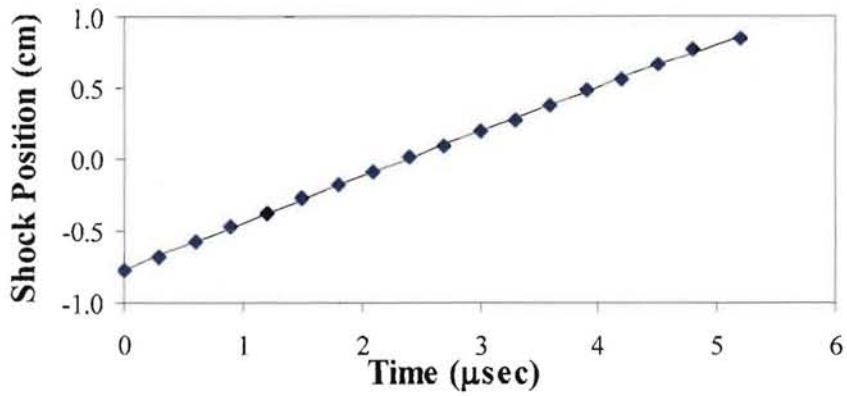

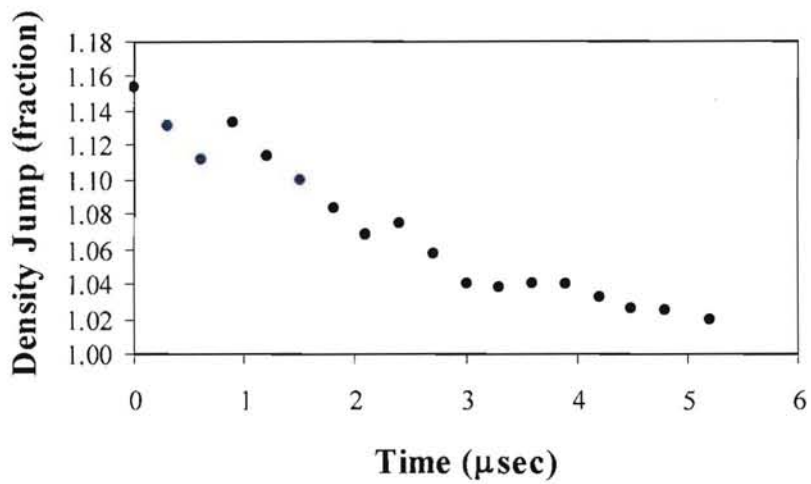

Single experiment, Multiple Measurements

- Single experiment measures many Hugoniot points
- Agreement with LASL Hugoniot data
- Hugoniot points measured from peak shock velocity down to nearly sound velocity

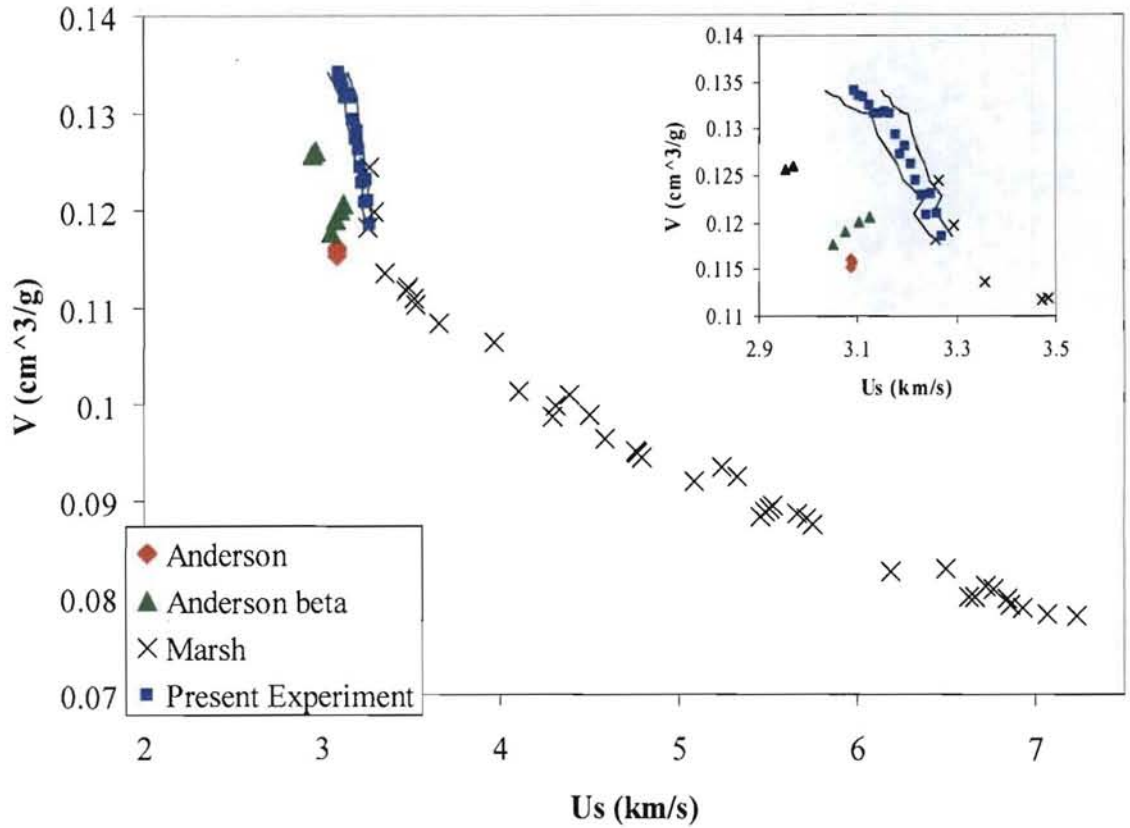

Thank you for listening

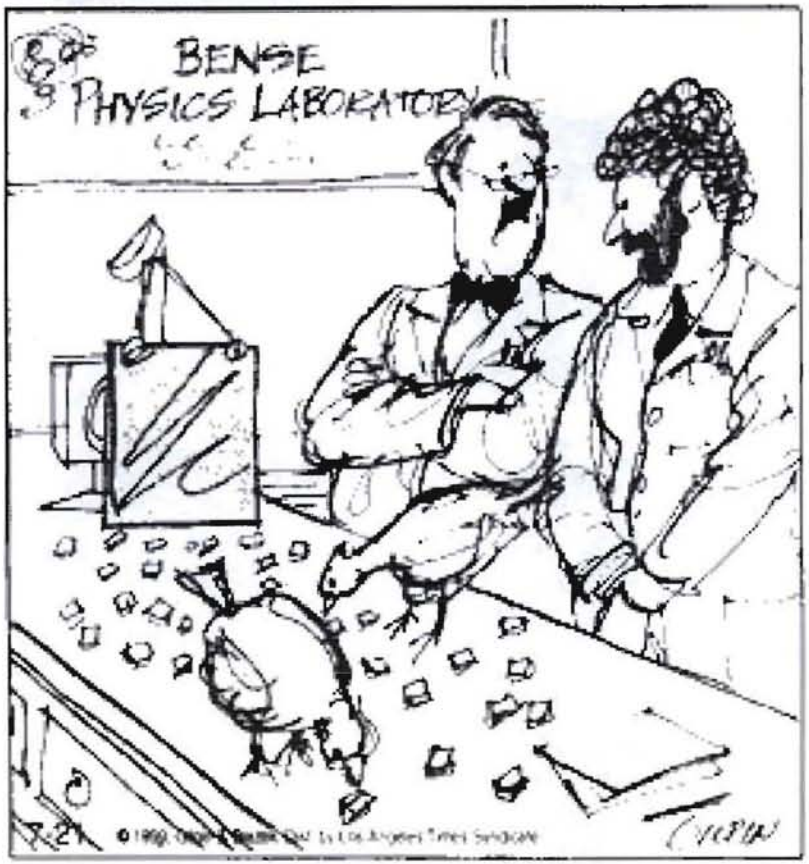

"Okay. Now that we know bombarding the sample with *croutons* isn't the answer, what say we try protons."

Protons have two key advantages over neutral particles:

1) They can be transported away from the object
2) Many intense pulses can be generated